

Alma Mater Studiorum – Università di Bologna

**DOTTORATO DI RICERCA IN
SCIENZE BIOMEDICHE
PROGETTO N°5: SCIENZE MORFOLOGICHE UMANE E
MOLECOLARI**

Ciclo XXIV

Settore Concorsuale di afferenza: BIO/16

**THE REGULATION OF SATELLITE CELLS DURING
SKELETAL MUSCLE REGENERATION AND
NEUROMUSCULAR DISEASE**

Presentata da: ANNARITA SCARAMOZZA

Coordinatore Dottorato

Relatore

Chiar.mo Prof. Lucio Cocco

Chiar.ma Prof.ssa Anna Maria Billi

Esame finale anno 2012

SUMMARY

INTRODUCTION	<i>pag.</i>	<i>1</i>
1. The Adult Skeletal Muscle Tissue: functions and characteristics	<i>pag.</i>	<i>1</i>
2. The Skeletal Muscle Regeneration	<i>pag.</i>	<i>4</i>
<i>Degenerative phase</i>	<i>pag.</i>	<i>4</i>
<i>Regenerative phase</i>	<i>pag.</i>	<i>5</i>
3. Skeletal Muscle Satellite Cells (SCs)	<i>pag.</i>	<i>8</i>
<i>Identification, distribution and characterization</i>	<i>pag.</i>	<i>8</i>
<i>Cellular and molecular control of SCs-lineage progression</i>	<i>pag.</i>	<i>11</i>
4. Changes in muscle SCs during Muscle Disease and Aging	<i>pag.</i>	<i>14</i>
4.1 Amyotrophic Lateral Sclerosis (ALS) and the possible Skeletal Muscle involvement	<i>pag.</i>	<i>15</i>
4.2 Role of P16Ink4a in cell cycle and tissue regeneration	<i>pag.</i>	<i>18</i>
<i>Cell Cycle progression through positive and negative regulators</i>	<i>pag.</i>	<i>18</i>
<i>p16^{INK4a}-pRB pathway, senescence and aging</i>	<i>pag.</i>	<i>21</i>
<i>The regulation of INK4a/ARF/INK4b expression</i>	<i>pag.</i>	<i>22</i>
AIMS OF THE PROJECTS	<i>pag.</i>	<i>25</i>
• PROJECT 1: <i>Isolation and characterization of Satellite Cells (SCs) from patients affected by Amyotrophic Lateral Sclerosis (ALS)</i>	<i>pag.</i>	<i>25</i>
• PROJECT 2: <i>The role of P16^{Ink4a} in skeletal muscle regeneration</i>	<i>pag.</i>	<i>26</i>

PROJECT 1	<i>pag.</i> 27
• RESULTS	<i>pag.</i> 27
• FIGURES	<i>pag.</i> 30
• DISCUSSION	<i>pag.</i> 39
• EXPERIMENTAL PROCEDURES	<i>pag.</i> 42
PROJECT 2	<i>pag.</i> 46
• RESULTS	<i>pag.</i> 46
• FIGURES	<i>pag.</i> 54
• DISCUSSION	<i>pag.</i> 70
• EXPERIMENTAL PROCEDURES	<i>pag.</i> 75
REFERENCES	<i>pag.</i> 81
ACKNOWLEDGMENTS	<i>pag.</i> 88

INTRODUCTION

1. The Adult Skeletal Muscle Tissue: functions and characteristics

The primary functions of the skeletal musculature are locomotor activity, postural behavior and breathing. Moreover, the muscle tissue is a primary site for glycogen storage, insulin uptake and amino acid catabolism, playing a crucial role in metabolism and heat production, through the contraction of muscle fibers. Skeletal muscle is composed predominantly of post-mitotic, multinucleated muscle fibers which are formed during development by fusion of mononucleated muscle progenitors originating from the somite. Muscle fibers, the basic contractile units of skeletal muscle, are individually surrounded by a thin connective tissue layer (*endomysium*) and grouped into bundles within the *perimysium*. The whole skeletal muscle is wrapped by a dense layer of connective tissue, called *epimysium* (Figure 1). Skeletal muscles are highly vascularized to provide essential nutrients for muscle functions and innervated to ensure muscle fiber contraction. A single motor neuron contacts a mature myofiber, which express different MHC isoforms and metabolic enzymes. Each muscle fibers is surrounded by the *sarcolemma* (plasma membrane) and has a cytoplasm called *sarcoplasm*, with numerous mitochondria, sarcoplasmic reticulum and myofibrils (Figure 1). Myofibrils, long protein bundles (1 μ m diameter), are composed by the myofilaments of *myosin* and *actin*, which constitute the *sarcomere*, the unit of the muscle contraction. The actin filaments are associated with other important regulatory proteins, such as *troponin* and *tropomyosin*, which are necessary for muscle contraction. Skeletal muscle cells are excitable and are subject to depolarization by the neurotransmitter acetylcholine, released at the neuromuscular junction by motor

neurons. The basic mechanism of muscle fibers contraction results from the “sliding mechanism” of the myosin-rich thick filaments over the actin-rich thin filaments after neuronal activation. Once a cell is sufficiently stimulated, the sarcoplasmic reticulum releases ionic calcium (Ca^{2+}), which then interacts with the regulatory protein troponin. Calcium-bound troponin undergoes a conformational change that leads to the movement of tropomyosin, subsequently exposing the myosin-binding sites on actin. This allows for myosin and actin ATP-dependent cross-bridge cycling and shortening of the muscle. The connective tissue combines the contractile myofibers into a functional unit, in which the contraction of myofibers is transformed in movement via myotendinous junctions at their ends, where myofibers attach to the skeleton by tendons.

Individual adult skeletal muscles are composed by a mixture of myofibers with different physiological properties: slow-contracting/fatigue resistant type, fast-contracting/non-fatigue resistant type. The proportion of each fiber type within the muscle controls the contractile property of muscle . Different signaling pathways and myoblast populations are involved in the early fiber type differentiation, which is established during early development. At the later stages, motor neurons and hormones play a fundamental role in determining the fiber type, even if individual muscles still retain an intrinsic commitment to form particular fiber types [1].

The terminally differentiated muscle fiber is not a fixed unit but can undergo change in fiber type (fast-to-slow or slow-to-fast switch) or fiber size (atrophy/hypertrophy). Muscle fibers can also repair local damages caused by eccentric contraction (i.e. lengthening) without obvious changes in myofibers and surrounding tissues and do not involve inflammatory response. However, more severe injuries resulting from traumatic lesions or from indirect causes such as neurological dysfunction or innate genetic defects, activate a finely orchestrated set of cellular responses, resulting in the regeneration of a well-innervated and fully vascularized skeletal muscle tissue.

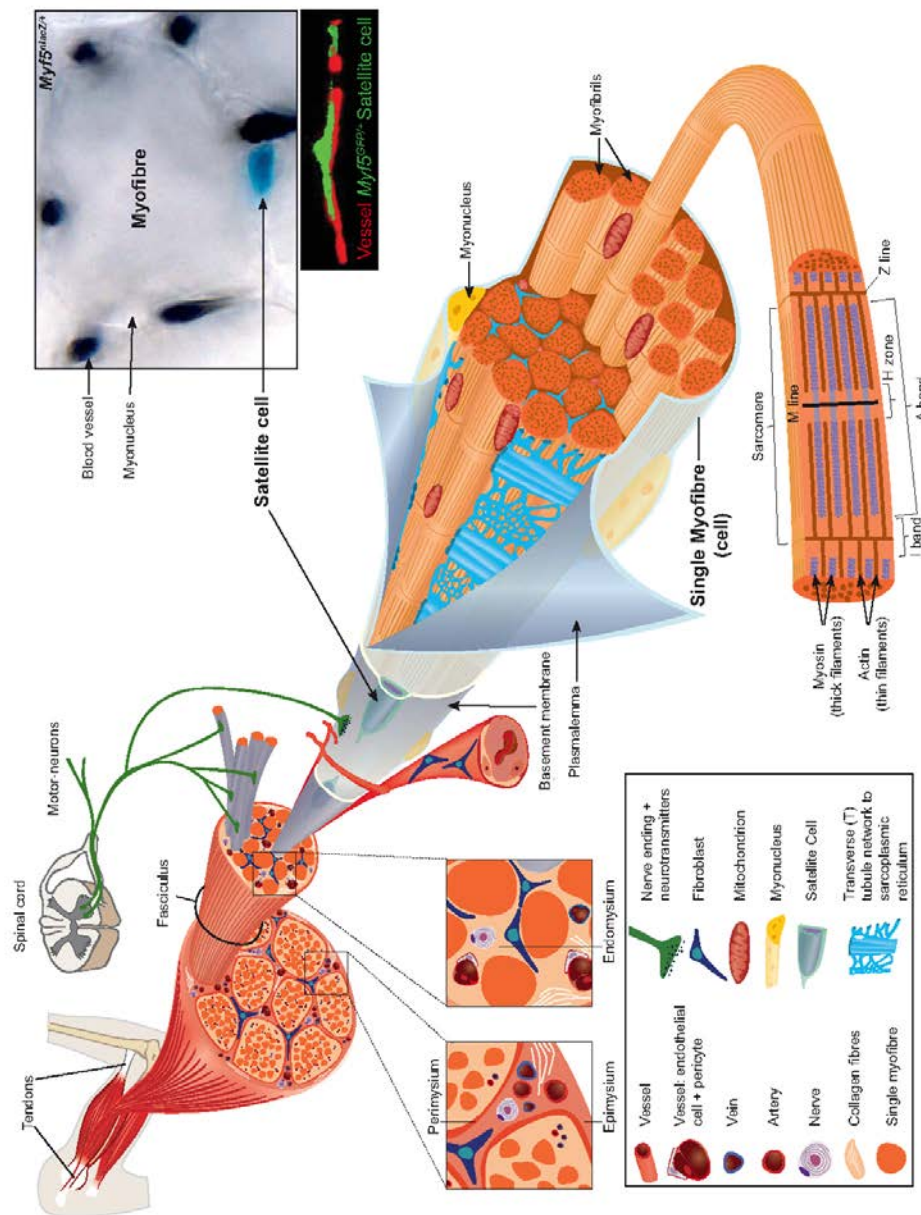


Figure 1. Scheme of skeletal muscle and associated structures. Three connective tissue layers can be distinguished in skeletal muscle. The epimysium is the deep fascia component that wraps the entire muscle and it is contiguous with the tendon (muscle to bone) and endosteum (fascia surrounding bone). The *perimysium* ensheaths individual muscle fibres into fasciculi (bundles). The *endomysium* is located between fibres and it ensheaths individual muscle fibres. The muscle cell (myofibers) are characterized by the presence of the *sarcoplasmic reticulum*, the major intracellular source of calcium needed for muscle contraction, which connects to the *transverse (T) tubules*, and these surround the *sarcomeres*. *Satellite cells* (SCs) are located between the basement membrane and the-plasmalemma of the myofibre. Image in upper right is a section of the tibialis anterior muscle of a mouse that was perfused-with India ink to label the vasculature and stained with X-gal to reveal SCs in a Myf5nlacZ adult mouse [2].

2. The Skeletal Muscle Regeneration

Skeletal Muscle possesses the remarkable capacity to complete a rapid and extensive regeneration, even following severe damage. The regenerative ability of skeletal muscle relies on Satellite Cells (SCs). SCs are located between the sarcolemma and the basal lamina of muscle fibers (Figure 1, 2).

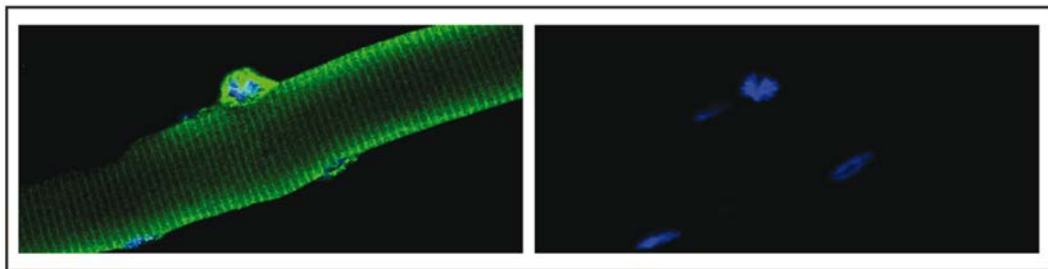


Figure 2. Satellite Cells (SCs). Fluorescence microscopic image of a mitotic SCs (metaphase) on a mouse muscle fiber. SCs is labeled by the expression of a yellow fluorescent protein and DNA is stained in blue [3].

In response to injury, SCs proliferate and differentiate to either fuse with existing myofibers or with other myogenic cells to generate new muscle fibers. The program of SCs activation and differentiation recapitulates in some way embryonic myogenesis, even if the regulatory mechanisms and the microenvironments in the two contexts are different.

Muscle regeneration consists of two different phases: the degenerative phase characterized by a massive inflammatory reaction and the regenerative phase, defined by the activation of SCs and the maturation and remodeling of regenerated muscle.

Degenerative phase

The inflammatory reaction. The muscle fiber necrosis represents the first event in the regeneration process, leading to a dissolution of the myofiber sarcolemma with consequent calcium influx and activation of calcium-dependent proteases, such as calpains that can cleave myofibrillar and cytoskeletal proteins [4]. The

disruption of muscle fibers integrity is reflected by increased serum levels of muscle proteins. For example, creatine kinase, which is usually restricted to the myofiber cytosol, is increased in human and animal models after mechanical stress and in the course of muscle degenerative diseases [5]. Neutrophils (defined by Ly6C⁺/F4/80⁻) represent the first myeloid cell population that appear after the acute muscle injury, with a significant increase in number within 2 hours after muscle damage, peaking in concentration between 6 and 24h and then they rapidly decline. After the neutrophil infiltration approximately, 24h post-injury, early phagocytic macrophages (CD68⁺, CD163⁻) become the major inflammatory cell population within the injured site until ~2 days post injury when their numbers start to decline. Macrophages secrete pro-inflammatory cytokines such as Tumor Necrosis Factor α (TNF α) and interleukin 1 β (IL-1 β) to promote/control/influence phagocytosis of necrotic tissue. Then, non-phagocytic macrophages (CD68⁻/CD163⁺) increase, reaching their peak at 2 to 4 days after injury and their number remains elevated for many days. They secrete anti-inflammatory cytokines that contribute to switch off the inflammatory response. This phase gives way to the regenerative phase of myogenesis.

Regenerative phase

Activation of SCs and maturation/remodeling of new regenerated muscle. Following injury, SCs are activated and undergo rapid proliferation starting ~ 48 hours after injury. Myogenic cells differentiate and fuse to existing fibers or together to generate new fibers.(Figure 3A).Normally, large number of new myofibers are formed in few days after muscle damage. Early studies proposed that new muscle fibers are generated via budding of myotubes from existing, injured fibers. However, it has been supported by several experimental evidences that this rapid repair occurs through the activation and differentiation of SCs, which represent the major candidate for the source of myogenic cells for muscle repair during injury-induced regeneration. Multinucleated myotubes could indeed be generated *in vitro* from single myogenic precursor cells, derived from muscle SCs [6-8]. *In vivo* transplantation-based approaches highlighted the regenerative potential of SCs. Donor SCs can be transferred into muscle of

injured or diseased mice and they are able to contribute extensively to the formation of new muscle fibers, in some cases engrafting the majority of fibers in the transplanted muscle. Transplantation into dystrophic mouse muscle of a single muscle fiber that contained as few as seven SCs led to an increasing number of new SCs that in turn generated more than 100 new muscle fibers and could also be activated after injury [9]. In addition, skeletal muscle precursor cells derived from SCs, can contribute to up to 94% of myofibers, restoring dystrophin expression and significantly improving muscle histology and contractile function in dystrophic-deficient mdx mice [10]. More directly, Sacco et al (2008) showed that a single muscle stem cell can be transplanted in a host injured muscle and it is capable alone of extensive proliferation, contributing to muscle fibres regeneration and repopulation of the SC pool [11]. This was first demonstration that a SC displayed stem cell character. In summary, SCs represent the most important and efficient source for repair of extensive muscle injury preserving the regenerative capacity of skeletal muscle throughout life.

During the regeneration process several factors are involved in the subsequent growth of regenerated muscle: involvement of blood vessels and re-establishment of neuromuscular and myotendinous connections. A morphological hallmark of regenerated muscle is the presence of myofibers of small caliber with centrally located nuclei (Figure 3B). New generated myofibers are generally basophilic and express embryonic/developmental forms of MHC, reflecting *de novo* fiber formation [12]. Once the fusion of myogenic cells is completed, newly generated myofibers increase in size and myonuclei migrate at the periphery of the fibers. Thus, under normal circumstances a regenerated muscle is morphologically and functionally undistinguishable from undamaged muscle.

Nonetheless, during aging or under several pathological conditions, the ability of skeletal muscle to fully regenerated is compromised. Several factors can affect the intrinsic property of the skeletal muscle tissue to regenerate, leading to the generation of abnormal muscle fibers. Indeed, regenerating myotubes, which reside in the same basal lamina, may not fuse together leading to the formation of cluster of small fibers, or they can give rise to forked fibers, due to the fusion

only at one extremity (*fiber splitting*). After segmental necrosis, SCs can proliferate and fuse at the damaged site, giving rise to appearances as “budding”. Scar tissue formation can prevent the reconstitution of myofiber integrity leading to myotendinous junctions.

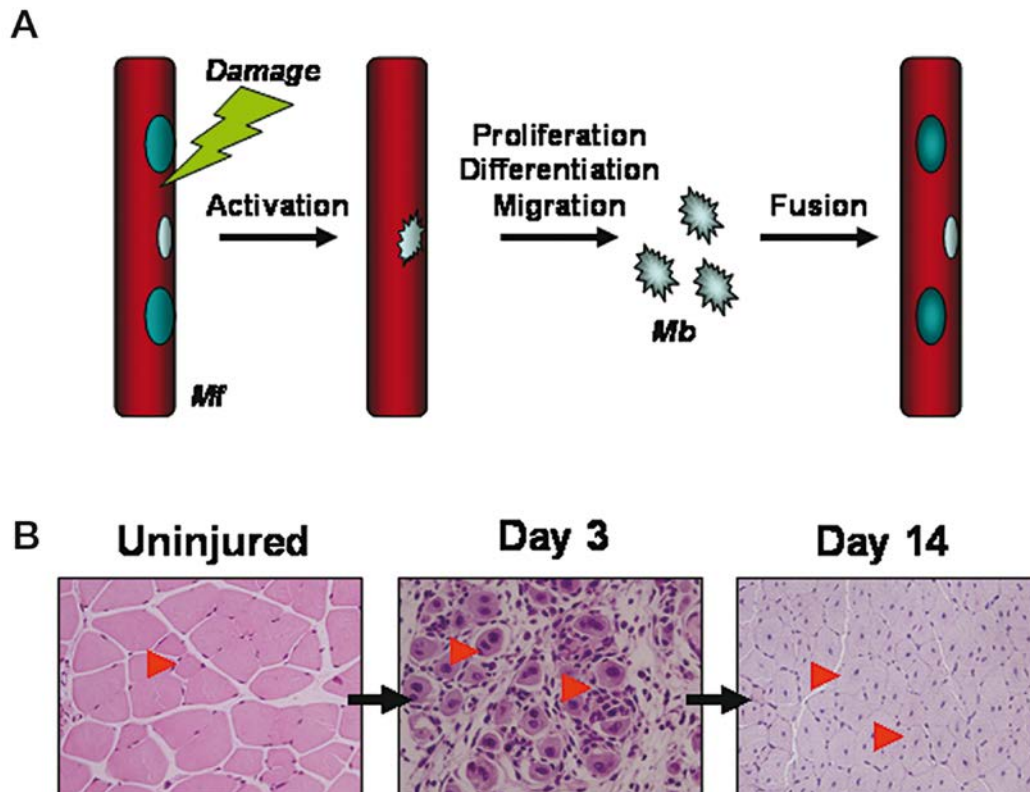


Figure 3. Skeletal Muscle regeneration. A. Muscle repair is mediated by myofibers (Mf) resident SCs (light blu).After damage activated SCs proliferate as myoblasts (Mb), differentiate and migrate in order to fuse each other to repair muscle. B. H&E staining shows uninjured and regenerating muscle after 3 and 14 days regeneration. Normally, muscle is characterized by peripherally located nuclei (red arrowhead). Three days after injury, muscle shows extensive inflammatory infiltrate and some small regenerating fibers with characteristic centrally located nuclei. At 14 days, the muscle is fully repaired, but regenerated fibers are still distinguishable by their central nuclei [13].

3. **Skeletal Muscle Satellite Cells (SCs)**

Identification, distribution and characterization

Skeletal muscle SCs have long been considered as a population of muscle-specific adult stem cells that are the major contributor to the postnatal maintenance, growth, repair and regeneration of the skeletal muscle tissue [14]. This population of adult stem cells was described for the first time by Alexander Mauro in 1961. He observed and identified by electron microscopy a population of mononucleated cells located in a “satellite” position between the basal lamina and the sarcolemma of frog muscle fiber [15]. He supposed that these cells were dormant embryonic myoblasts that recapitulate the embryonic muscle development after injury. Indeed, during development, the SCs originate from paraxial mesoderm-derived cells of the dorsal somites [16]. These cells are specified by signals from neighboring cells of the notochord, neural tube and dorsal ectoderm through the action of transcription factors such as the paired box proteins Pax3 and Pax7 [17-18]. Once committed, somite-derived cells migrate to multiple sites of embryonic myogenesis, express the myogenic basic helix-loop-helix transcription factors (MRFs) Myf-5 and MyoD [19] and differentiate into muscle fibers. Pax3 and its paralogue Pax7 have been implicated in the specification of cells that will enter the myogenic program. In the absence of both Pax3 and Pax7, there is a major deficit in skeletal muscle, with arrest of myogenesis occurring during later embryonic and fetal development [20]. Pax3 is required for the establishment of limb muscles and the migration of embryonic precursors from the somites to the limbs [20]. Instead, Pax7 is dispensable for prenatal muscle formation but it is required for normal postnatal muscle growth [21-22]. Moreover, Pax7 is present in adult SCs, and in its absence muscle regeneration is severely affected. SCs were not observed in the mutant, leading to the proposal that Pax7 is also essential for the specification of adult muscle progenitor cells [21]. Somite-derived myogenic progenitors that do not differentiate into myofibers at this time have been suggested to form the adult SC pool. Several *in vitro* and *in vivo* studies support Pax7 critical role in adult

muscle stem cells [22-26]. Genetic lineage tracing approaches shown that the majority of all adult quiescent SCs expressed at some point during their development the MRFs Pax3, Myf5, MyoD and Pax7 [26-29].

The muscle progenitors give rise to specialized muscle fiber associated SCs. They are found beneath the basal lamina and adjacent to the plasma membrane of mature muscle fibers [15] and first appeared in the limb muscles of mouse embryos at E16-18. SCs are most abundant early in life in neonatal mice and SCs nuclei comprise approximately 30% of myofibers-associated nuclei. However, SCs number declines with age, and only about 5% of myofibers nuclei in the muscles of adult mice represent SCs [30]. Adult SCs reside in a quiescent state within the basal lamina surrounding individual muscle fibers. This well-defined anatomical niche protects SCs from the external environment, even if the SCs are capable to respond to external perturbation. In this dormant state, they are characterized by a high nuclear-to cytoplasmic ratio, reduced organelle content and a smaller nucleus size with increased amount of heterochromatin compared to fiber myonuclei [31].

SCs can be identified by numerous markers [32]. The most useful marker, Pax7 uniformly marks adult SCs. Numerous works have shown how to isolate and functionally characterize myogenic subpopulations of myofibers-associated cells, using various combinations of markers: $\alpha7$ -integrin⁺CD34⁺ [11], Myf5Cre⁻, $\alpha7$ -integrin⁺ $\beta1$ integrin⁺ [33], syndecn3/4⁺ [34], CXCR4⁺, $\beta1$ integrin⁺ CD45⁻, Mac1⁻, Sca1⁻ [10]. Nonetheless, all these population of muscle stem cells, that maybe represent a subset of a common pool of muscle SCs, express Pax7. This transcription factor was first described by Seale et al (2000) as a marker of SCs and is essential for their specification and expansion [20-22]. Then, its expression is downregulated when SCs commit to muscle differentiation. By lineage tracing experiments, Lepper et al. showed that Pax7 expression marks adult stem cells in injury-induced myogenesis *in vivo* [26]. Moreover, Shea et al. demonstrated for the first time that Pax7Cre derived cells contribute to myofibers differentiation and fully restore the renewed SCs pool back to homeostasis during repair [35]. However, it seems that there is a cell intrinsic

difference between neonatal progenitors and adult SCs in their Pax7 dependency. Pax7 is required for myogenic function within the early postnatal growth period but dispensable for repair. Indeed, when Pax7 is inactivated in adult mice, mutant SCs are not compromised in muscle regeneration, they can proliferate and reoccupy the sublaminar satellite niche, supporting further regenerative process. [26]. These recent findings highlight the differences between adult and embryonic/post natal SCs. However, the heterogeneity in gene expression and myogenic potential in the population of SCs, and the findings that many other stem cells can contribute to muscle regeneration arise the question if Pax7⁺ SCs represent the major cell type involved in muscle repair. Bone marrow derived progenitors [36], skeletal muscle side populations [37], mesangioblasts [38], pericytes [39-40], CD133(Prom1)⁺ progenitors [41], PW1(Peg3)⁺ interstitial cells [42] have been showed to incorporate into newly formed myofibers. In addition, fibroblastic/adipogenic mesenchymal progenitors (FAPs) interact with SCs to regulate muscle homeostasis [43]. However, how much these cells can contribute to the normal physiological muscle repair remain still unclear. Recent significative works describe with different genetic ablation approaches that Pax7 expressing SCs are indispensable and required for adult skeletal muscle regeneration. Sambasivan et al (2011), used a knock in Pax7^{DTR} mouse model, which express a diphtheria toxin DT receptor (DTR) under the control of Pax7 gene promoter. The intramuscular administration of DT, potent inhibitor of protein translation, ablate all Pax7^{DTR+} cells, leading to a marked loss of muscle tissue and failure to regenerate skeletal muscle. In addition, skeletal muscle become infiltrated by inflammatory cells and adipocytes [44]. In the other study by Lepper et al (2011), they used Pax7Cre^{ER} in combination with R26R^{eGFPDTA}. In this model with the injection of tamoxifen all Pax7⁺ cells will express the diphtheria toxin fragment A (DTA) which mediates cell autonomous killing. They found that the elimination of Pax7⁺ cells completely blocks the regeneration after TA injury and after transplantation of EDL muscle into nude mice [45]. In the last work, Murphy et al (2011) used Pax7^{CreERT2} and Tcf4^{CreERT2} crossed with R26R^{DTA} mice to genetically ablate SCs and fibroblasts. The ablation of SCs resulted in a complete loss of regenerated muscle, as well as

misregulation of fibroblasts and dramatic increase in connective tissue. Instead, the fibroblasts ablation causes premature differentiation of SCs, depletion of the early pool of SCs and smaller regenerated fibers [46]. Therefore, all these results showed that SCs are required for skeletal muscle regeneration and the loss of SCs is not compensated by other stem cell types. Muscle regeneration, indeed, was rescued after transplantation of only adult Pax7⁺ cells [44]. Other cell types which possess regenerative potential are strictly dependant on the presence of SCs.

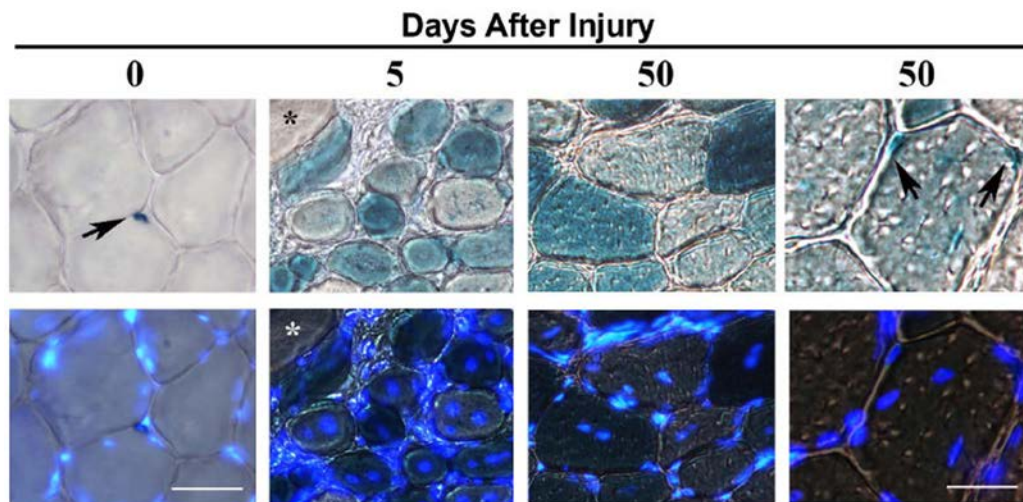


Figure 4. Pax7SCs are capable to self renewal and contribute to muscle regeneration. Pax7⁺/XGal⁺ SCs in muscle of *Pax7-CreERTm;R26R-lacZ* mouse reporter. Transverse sections show Pax7⁺/X-gal⁺ mononucleated cells in the SCs position of uninjured (0 days) and regenerated muscle fibers (50 days) (black arrows) [35].

Cellular and molecular control of SCs-lineage progression

Several works, with the use of inducible lineage tracing approaches, showed that after injury, quiescent adult Pax7⁺ cells become activated myoblast progenitors and they enter the cell cycle. Only a subpopulation of these cells come back to quiescence to replenish the SCs compartment, while others contribute to the new muscle fiber formation [26, 35].

The progression of activated SCs toward myogenic differentiation is controlled by the Myogenic Regulatory Factors (MRFs). They belong to a family of transcription factors that share a homologous basic helix-loop-helix (bHLH) domain responsible for DNA binding and dimerization with members of the E protein family. MRF-E protein dimers bind the E-box elements (CANNTG) found in the promoters of key muscle-specific gene [47]. Activated Pax7⁺SCs upregulate MyoD expression and proliferate to form myoblasts. Some of the Pax7⁺/MyoD⁺ cells return to quiescence through the downregulation of MyoD, a critical step of the reversion to quiescence. Indeed, it has been shown that Pax7, which is transcriptionally active during the quiescent state, is sufficient to promote the return to quiescence through repression of MyoD [24, 48-49]. The majority of the proliferating myoblasts progress toward the differentiation program characterized by the downregulation of Pax7 and the Myogenin upregulation. Finally, differentiated mononuclear myogenin⁺/MyHC⁺ (Myosin Heavy Chain) myocytes fuse together to form multinucleated myotubes or nascent myofibers (Figure 5).

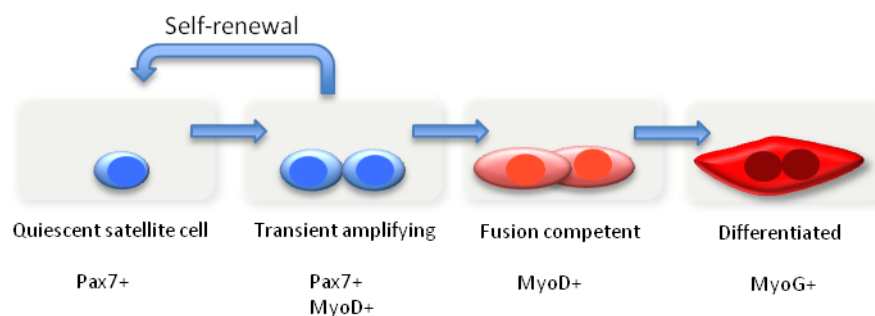


Figure 5. MRFs and myogenic lineage progression. Quiescent Pax7⁺SCs are activated and proliferate as Transient Amplifying Cells (TAC) characterized by the coexpression of Pax7 and MyoD. The majority of TAC pool follow the myogenic lineage progression becoming fusion competent cells characterized by the downregulation of Pax7. Finally, they are able to fuse and form differentiated multinucleated myotubes overexpressing Myogenin (MyoG). Some of the activated TA Pax7⁺/MyoD⁺ cells are able to self renew and reestablish the pool of quiescent SCs. (Courtesy of Andrew S. Brack).

The host fiber, as well the basal lamina, represent important factors for the SCs niche. For instance, it has been shown that mechanical, electrical and chemical signals originating from the host fiber can modulate the activity of SCs [14]. Furthermore, signals coming from the microvasculature and interstitial cells, such as macrophages, fibroblasts and muscle-resident stem cells also constitute an important component of the SCs niche (Figure 6). However, whether other resident cell population can control the SCs quiescence remains unclear. A number of different signaling pathways have been associated to the regulation of muscle SCs function such as Ang1/Tie-2, Notch, Wnt and Sonic Hedgehog pathway. Recently, HGF and Ang1 have been implicated as quiescence-inducing, ligand derived-growth factors [50-51]. Notch signaling controls quiescence and promotes stem cell fate decisions. Indeed, Notch3 is highly expressed in dormant Pax7⁺ SCs and proliferating SCs have high expression of Notch ligand Delta [52-53]. In addition, Notch signaling seems to inhibit myogenic differentiation through the upregulation of Numb, an inhibitor of Notch signaling. Then, a temporal balance between Notch and Wnt signaling controls the coordination from myoblasts to differentiated cells [54]. Many other factors have been identified to act by regulating SCs quiescence and activation, such as Fibroblast Growth Factors (FGF), Insulin Growth Factors (IGF), hepatocyte Growth Factors (HGF), Transforming Growth Factors β (TGF β) and Interleukin 6 (IL6) [55]. In addition, RTK (Receptor Tyrosine Kinase) are key mediator of grow factor signaling response, (i.e. FGF). Sprouty (Spry) represents a downstream target and negative regulator of RTK signaling. Recently, Shea et al (2010) showed that Spry1 is robustly expressed in quiescent SCs in uninjured adult muscle. Then, Spry1 expression is downregulated in activated SC after injury, and re-expressed as soon SCs go back to quiescence. They also showed that disruption of Spry1 using either inducible Pax7Cre^{ERTM} allele or a germline knockin approach reduces the pool of SCs that return to quiescence. Therefore, Sprouty1 plays a pivotal role in sensing growth factors within the environment and regulating SCs quiescence during muscle growth and repair [35, 56].

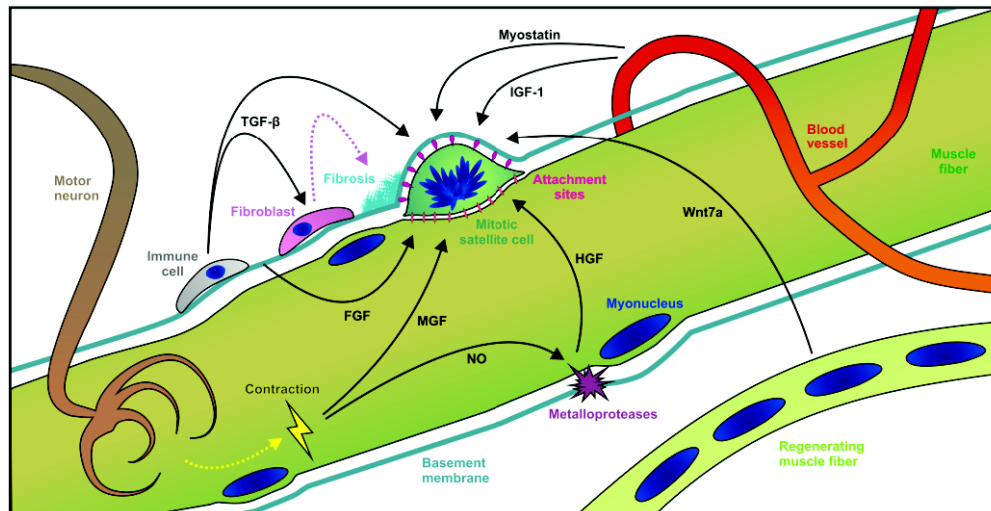


Figure 5. The SCs niche and regulatory factors. Schematic representation of the different environmental cues influencing SCs niche. FGF fibroblast growth factor; HGF hepatocyte growth factor; IGF, insulin-like growth factor; MGF mechano-growth factor; NO, nitric oxide; TGF, transforming growth factors [3].

4. Changes in muscle SCs during Muscle Disease and Aging

Several muscle pathological conditions, such as congenital myopathy, denervation, muscle atrophy, which are characterized by progressive loss of muscle mass and strength, may exhibit a decrease in the number and proliferative potential of SCs. The underlying mechanisms responsible for these changes of SCs pool and activity are still not completely understood. During chronic degenerative conditions, skeletal muscle undergoes through multiple bouts of regeneration and degeneration. In this context the repeated cycle of activation and proliferation of SCs may lead to telomere shortening or accumulation of mutations in specific SCs genes, resulting in SCs exhaustion. SCs exhaustion may also be related to frequent exposure to inflammatory conditions, oxidative stress. Moreover, non myogenic cells in the diseased muscle (i.e. fibroblasts) can affect muscle regeneration [57]. During aging there is a gradual decline in the regenerative potential of most tissue, due to a combination of age-dependent changes in the

environments and in the tissue specific stem cell. In aging skeletal muscle, damaged muscle fibers are less frequently regenerated by new fibers, leading to age-dependent loss of muscle mass and decline in strength, commonly referred as sarcopenia. Age-related deficits in muscle regeneration have been linked to functional decline in muscle SCs and their ability to repair skeletal muscle after injury [58-59]. Extrinsic change in aging muscle stem cells (i.e. Notch, Wnt signaling pathway) and intrinsic alteration can affect the regenerative ability of SCs. Indeed, the lack of SCs entering the cell cycle, and the exposure to an oxidative and inflammatory stress, makes SCs more susceptible to accumulation of cellular and genotoxic insults. In the aging context stem cells also can go through the senescence process upregulating the tumor suppressor gene and cell cycle inhibitor p16Ink4a. P16Ink4a expression has been described in several tissue from aging mice and human, as well it has been correlated with replicative decline in the HSC and NSC compartments [60].

4.1 Amyotrophic Lateral Sclerosis (ALS) and the possible Skeletal Muscle involvement

Amyotrophic Lateral Sclerosis (ALS) represents the most common form of the adult-onset motor neuron diseases (MND). ALS, first described by the French neurobiologist and physician Jean-Martin Charcot, is a fatal neurodegenerative disorder that mainly affects pyramidal neurons in the motor cortex and lower motor neurons (MNs) that originate in the brainstem and spinal cord. The name of the disease reflects the different tissue compartments that are severely affected. In particular, *amyotrophic* refers to the atrophy of the skeletal muscle fibers and loss of muscle mass; *lateral* refers to nerve tracks that run down both sides of the spinal cord; *sclerosis* reflects the scar tissue that remains after MNs degeneration

The most typical feature of this progressive lethal disease is the selective and premature degeneration and death of cortical and spinal MNs leading to the clinical characteristics of muscle weakness, fasciculations, muscle atrophy,

speech and swallowing disabilities, progressive paralysis, and death caused by respiratory failure, which usually occurs within 2-5 years of disease onset depending on the severity and the stage of disease when diagnosed.

Although the majority of incidences have no apparent hereditary contribution and are, hence termed sporadic, the remainder (~10%) are of genetic origin, generally transmitted with an autosomal dominant inheritance [61]. During these years several genes have been studied and linked to familial ALS (fALS), including *angiogenin*, *vapb*, *dynactin*, *tdp43*, *fus/tls*. However, how the mutation of these genes trigger ALS is still unknown [62-64]. A landmark discovery reported in 1993 initiated the molecular era of ALS research with identification of mutations in the gene encoding the superoxide dismutase 1 (SOD1) as causative in 20% of the inherited cases [65]. SOD1 normally functions as an enzyme involved in oxidative stress resistance, converting highly reactive superoxide to either hydrogen peroxide or oxygen. There is convincing evidence that mutant SOD1 (mSOD1) kills MNs because of a neurotoxic property (gain of function hypothesis) rather than a deficiency in dismutase activity (loss of function hypothesis) [64]. However, the pathophysiological mechanisms of ALS are still elusive. A number of mechanisms have been proposed by which mSOD1 leads to MNs cell death, including the following: misfolding of the mutant protein, interference with axonal transport or cytoplasmic trafficking, altered oxidative activity of the mutant enzyme, a defect in the EAAT2 glutamate transporter leading to excitotoxicity [66]. Nonetheless, recent works highlighted the fact that MNs are not the only cell type involved in ALS pathogenesis, challenging these “neurocentric” view. Other cell types, such as glial cells and skeletal myofibers, seems to participate in the triggering of MNs degeneration [63, 67-68]. Indeed, the first event in the disease process in mSOD1 mice is the interruption of the nerve connection at the neuromuscular junction (NMJ), followed by axonal degeneration and death of MNs cell bodies [69].

The controversial discussion still continues as to what extent muscle denervation in ALS models is of neuronal origin. Neuron-restricted expression of mSOD1 does not recapitulate the hallmarks of the disease [70-71], possibly due

to low mSOD1 expression levels [72]. Involvement of skeletal muscle in ALS pathophysiology was first understood from early muscle hypermetabolism in mSOD1 mice and human patients [73-74]. Moreover, it has been found that the neurite outgrowth inhibitor Nogo-A is strongly expressed in ALS skeletal muscles [75]. Recent studies provide evidence that skeletal muscle-specific mSOD1 overexpression is sufficient to induce muscle atrophy and oxidative damage and trigger key features of ALS in spinal cord such as astocytosis and inflammation, as well as MNs degeneration [68, 76]. Williams AH et al (2009) reported that miR-206, a microRNA specifically expressed in the skeletal muscles, delays ALS progression and promotes regeneration of neuromuscular synapses in mouse models. Indeed, loss of miR-206 accelerates disease progression and atrophy of skeletal muscle, leading to kyphosis, paralysis and death [77].

All this evidence reinforce the hypothesis that skeletal muscle appear to be involved in ALS pathogenesis in conjunction with other cell types. It is well known that the connection between muscle and nerve is crucial for both cell types in order to survive and function throughout the life (Figure 1). Moreover, skeletal muscle is also a source of signals that influence neuron survival, axonal growth and maintenance of synaptic connections [78]. Indeed, the development in absence of skeletal muscle results in the sequential ablation of MNs from the spinal cord to the brain [79]. Thus, skeletal muscle plays a crucial role in providing guidance and cues to the developing MNs, and sustain a trophic support for the maintenance of MNs and the axon function. On the other side, the first stages of muscle regeneration after injury and the activation, proliferation, differentiation and fusion of SCs, can take place in the absence of nerves. However, their presence is fundamental for growth and maturation of newly formed myofibers, which in absence of neural activity remain atrophic. The role of nerve activity in muscle regeneration is demonstrated in rat soleus muscle after muscle injury induced by bupivacaine injection. Bupivacaine causes the necrosis of all soleus muscle fibers, leaving SCs, nerve terminals, as well as blood vessels, intact. After 3 days of regeneration both the innervated and the denervated muscles are composed of thin myotubes expressing embryonic

MyHC. The innervations process starts approximately at day 3 after injury [80-81]. Three days after injury, denervated regenerating myofibers do not display further growth, compared to the innervated muscles.

Although the denervation of NMJ in ALS is clear, the potential alteration in myogenic regulation remain unexplored. Indeed, muscle autonomous mSOD1 toxicity may limit the capacity of mutant muscle to regenerate, modifying the activity of SCs and the MRF molecular regulation. It seems, indeed, that SCs isolated from ALS patients are affected in their capacity to proliferate and differentiate. Pradat et al, (2011) showed that the dividing myoblasts *in vitro* exhibited abnormal morphological features reminiscent of senescent cells. Moreover, during differentiation, these cells form long thin myotubes with weaker MHC isoform expression [82]. Nonetheless, more studies are required in order to understand whether SCs abnormalities or defects in the program of muscle differentiation and maturation in ALS may be a part of the non-cell-autonomous process.

4.2 Role of P16Ink4a in cell cycle and tissue regeneration

Cell Cycle progression through positive and negative regulators

During the early process of skeletal muscle differentiation, MRFs are involved not only in the control and regulation of muscle specific genes, but also in modulating the transition from quiescent SCs, to Transient Amplifier Cells (TAC) towards differentiated myotubes. This transition requires cell cycle withdrawal during the G1 phase. Along cell cycle progression, and in particular in G1 phase, checkpoints are encountered. Depending on the ability to pass these points, the cell will determine its fate. Indeed, cells can enter in a reversible quiescent state (G0), or differentiate in a more specialized non-proliferating cells. Cells can become senescent, metabolically active, but in a permanently retired state or lastly, they can go through apoptotic mechanisms and die. Therefore, it is clear that there is an extremely fine crosstalk and balance between MRFs and cell cycle regulators during myogenesis [83-84].

The G1 cell cycle phase is controlled at the molecular level by several positive and negative regulators. In particular, among the positive regulators there are cyclins and cyclin-dependent kinases (CDKs) (Figure 6). The CDKs belong to the class of protein serine-threonine kinases and depend on the binding of a cyclin in order to become activated by a CDK-activating kinase. Then, the activated Cyclin-CDK complexes are able to phosphorylate downstream targets, such as cell cycle repressors. Cyclin D is one of the major regulators of G1 phase progression. After mitogen stimulation, Cyclin D is upregulated in the early phase of G1. The association of Cyclin D with CDK4 or CDK6, lead to the phosphorylation of the retinoblastoma protein, Rb. Rb functions as a tumor suppressor gene. Indeed, in hypophosphorylated state it is active and repress cell cycle progression by inhibiting E2F transcription factors. Therefore, the CyclinD/CDK4/6-mediated phosphorylation of Rb causes the release of Rb from E2F, which is now available for the transcription of late G1/S phase genes.

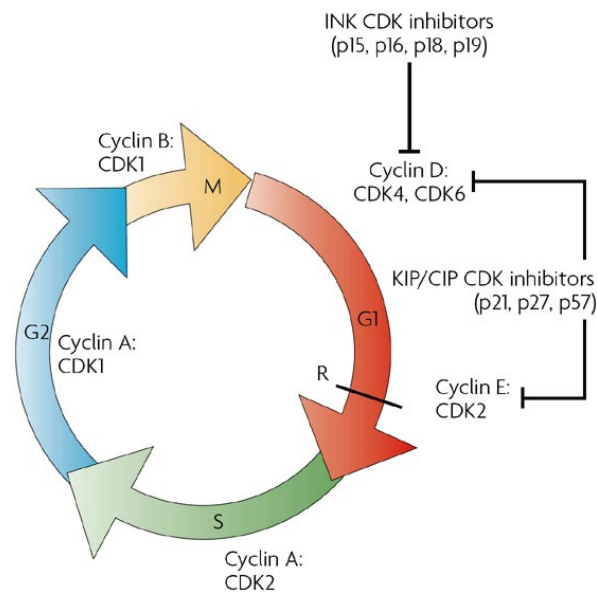


Figure 6. Cell cycle progression and G1 phase regulation. Diagram depicting the four phase of cell cycle and the cyclin/CDK complexes that are crucial for progression. Regulation of G1 phase by CDK inhibitors, cyclin/CDK complexes [85].

Cdk inhibitors (CKIs) and pocket proteins of RB family, such as p107 and p130 are negative regulators of cell cycle progression. The CKI cell cycle

inhibitors are divided in two families based upon their structure and cdk targets. The first group, known as the INK4 proteins bind specifically to inhibit the catalytic subunit of CDK4 and CDK6 and include p15, p16, p18 and p19. The second group, the Cip/Kip family, binds to cyclin D-, A- and E-dependant kinases via both cyclin and catalytic subunits and include p21, p27 and p57 [86] (Figure 6).

The locus *INK4a/ARF/INK4b* (also known as *CDKN2a* and *CDKN2b*) encodes three genes within 35kb: *ARF* (also known as *p19^{ARF}* and *p14^{ARF}*), *p15^{INK4b}* and *p16^{INK4a}*. Whereas *p15^{INK4b}* has its own open reading frame that is physically distinct, *p16^{INK4a}* and *ARF* have different first exons that are spliced to a common second and third exon. Even if *p16^{INK4a}* and *ARF* share both exon 2 and exon 3, the proteins are encoded in alternative reading frames. Therefore *p16^{INK4a}* and *ARF* are not isoforms and do not share any amino acid homology (Figure 7). The INK4 class of cell cycle inhibitors *p15^{INK4b}*, *p16^{INK4a}*, *p18^{INK4c}* and *p19^{INK4d}* (different from *p19ARF*) are homologous inhibitors of CDK4/6. The binding of the INK4 proteins to CDK4/6 induces an allosteric change that abrogates the binding of this kinase to Cyclin D, inhibiting the Rb phosphorylation. Both *p15^{INK4b}* and *p16^{INK4a}* are able to keep Rb-family proteins in a hypophosphorylate state, promoting the binding with E2F and the block of cell cycle progression at G1 [87-88] (Figure 7). During myogenic progression, pRb is maintained in inactive hyperphosphorylate state in cycling TAC and it becomes hypophosphorylate and active during myogenic differentiation, inhibiting E2F and leading to withdrawal from cell cycle. It has been shown that lack of pRb causes severe deficiency of skeletal muscle in newborn pups of *Rb1* knockout mice and when pRb is absent myoblasts show defect in terminal differentiation [89]. Recent work showed that loss of Rb1 specifically in SCs causes an increase in activated SCs but delay in terminal differentiation. Moreover, they observed smaller muscles of postnatal mice and delayed muscle regeneration after injury [90].

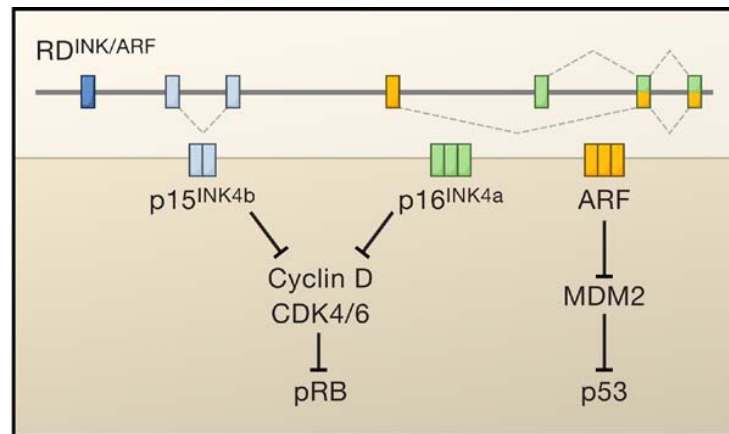


Figure 7. The *INK4a/ARF/INK4b* Locus The *INK4a/ARF/INK4b* locus encodes three genes within 35 kilobases: *ARF*, *p15^{INK4b}*, and *p16^{INK4a}*. Members of the INK4 family of cyclin dependent kinase inhibitors bind to and inactivate CDK4/6. ARF inhibits MDM2, resulting in p53 stabilization. RDINK/ARF indicates a newly discovered origin of replication 5' to *p15^{INK4b}* that participates in the transcriptional silencing of the *INK4a/ARF/INK4b* locus [87].

p16^{INK4a}-pRB pathway, senescence and aging

Tissue repair and regeneration are essential for longevity and often depend on the proliferation of stem or progenitor cells. In skeletal muscle, as other mammalian tissue, the regenerative capacity of resident stem cells declines with age. The stem cell population can ensure tissue repair and regeneration, but their hyperproliferative property can also drive cancer. Therefore, tumor suppressor mechanisms are fundamental in order to prevent malignant cell transformation by the activation of process such as apoptosis or senescence. p16^{INK4a} cell cycle inhibitor is considered also an important tumor suppressor functioning as a mediator of cellular senescence. Cellular senescence is an important mechanism to prevent the malignant progression of tumor cells. Senescent cells accumulate in various tissue and organs during aging and have been hypothesized to affect tissue structure and function [91]. Indeed, p16^{INK4a} expression has been associated with cancer and aging in mammalian systems and its expression has

been shown to markedly increases with age in the majority of all mammalian tissues [92]. Recently, Baker et al (2011) designed a novel mouse model with INK-ATTAC transgene for inducible deletion of p16^{Ink4a}-positive senescent cells. Basing on this approach they demonstrated that in the BubR1 mouse background, the removal of p16^{INK4a} – positive senescent cells upon drug treatment. delayed onset of these aging related phenotypes, such as. sarcopenia in skeletal muscle [93]. However, these results relies on BubR1 hypomorphic mice model, in which the physiological aging process is accelerated. Indeed, *BubR1* encodes a key member of the mitotic checkpoint, ensuring accurate chromosome segregation during mitosis. *BubR1* hypomorphic mice shows markedly shortened lifespan and prematurely exhibit a variety of age related phenotypes. Other important studies have demonstrated that increased p16^{INK4a} expression appears to play a role in the age-associated functional decline of the replicative potential of certain stem cell compartments, such as HSCs [94], pancreatic β -cells [95-96] and Neural Stem Cells (NSCs) [97]. Accordingly, p16^{INK4a} deletion attenuates the age-related decline in the repopulation potential of stem cells in these compartments [94, 97-98] and partially restores several age-related phenotypes in skeletal muscle and fat tissues in a premature aging mouse model (BubR1 insufficient) [99]. All these data suggest an uncover role for p16^{INK4a} tumor suppressor in promoting ageing. However, it remain still not clear how p16^{INK4a} drive stem/progenitor cell aging. It may promotes aging by inducing irreversible senescence arrest, or by a reversible quiescent state. Moreover, a caveat of these results is that they relied on germline inactivation or overexpression of p16^{INK4a}. Therefore, some of age-promoting effects of p16^{INK4a} expression observed in these systems may result from developmental compensation or non cell autonomous effects.

The regulation of INK4a/ARF/INK4b expression

p16^{INK4a} activation has been shown to be regulated both at transcriptional and post-transcriptional levels. MAPK signaling via ERK and p38MAPK has

been suggested to induce p16^{INK4a} expression in response to oncogenic activation or stress stimuli. Expression of p16^{INK4a} can be either transcriptionally activated (e.g. Ets family) or inhibited (e.g. Id proteins) by a number of pathways. Recently, some studies have suggested also a post-transcriptional regulation of p16^{INK4a} through interaction with microRNAs [100]. Additionally, a few repressors of *INK4a/ARF/INK4b* expression have been identified. In particular, the PcG (Polycomb Group) proteins, such as BMI1 and EZH2, have been shown to epigenetically silence p16^{INK4a} expression. PcG genes are epigenetic chromatin modifiers involved in heritable gene repression and maintenance of stem cell self-renewal and proliferation. For example, *Ezh2*, which belongs to the Polycomb Repressive Complex 2 (PRC2) is developmentally regulated in skeletal muscle and prevents myogenic gene transcription and differentiation [101]. Moreover, Juan AH et al (2011), showed that conditional ablation of *Ezh2* in SCs cause a reduction of the pool of Pax7⁺ cells and muscle mass leading to muscle regeneration defects [102]. Therefore, EZH2 controls self-renewal and proliferation of SCs, through the maintenance of an appropriate transcriptional program. *Bmi1* is another PcG that belongs to the PRC1 complex. *Bmi1* has been shown to play a crucial role in regulating cell cycle entry as well as maintaining self-renewal capacity of various adult stem cells. In particular, *Bmi1* deficient mice displays accelerated reduction of HSC [103] and reduced self-renewal of NSC [104]. Of note, the defects in HSC and NCS observed in absence of *Bmi1* are partially restored by deletion of *Ink4a/Arf*. Indeed, the action of *Bmi1* is in part, mediated through transcriptional repression of *Ink4a/Arf* locus, essential for G1/S cell cycle progression. By repressing CDK inhibitors of INK4 family, *Bmi1* and the other PcG proteins enable the activation of CyclinD/CDK4/6 complex and consequently progression through the G1 phase of the cell cycle [105]. *Bmi1* deficiency has been shown to not have any effect on the differentiation of skeletal muscle during embryonic and fetal stage [106]. However, it seems that *Bmi1* is required for SC maintenance and regeneration postnatally. Indeed, SCs from *Bmi1* knockout mice show reduced proliferative capacity and failure to re-enter cell cycle when exposed to high serum conditions [107].

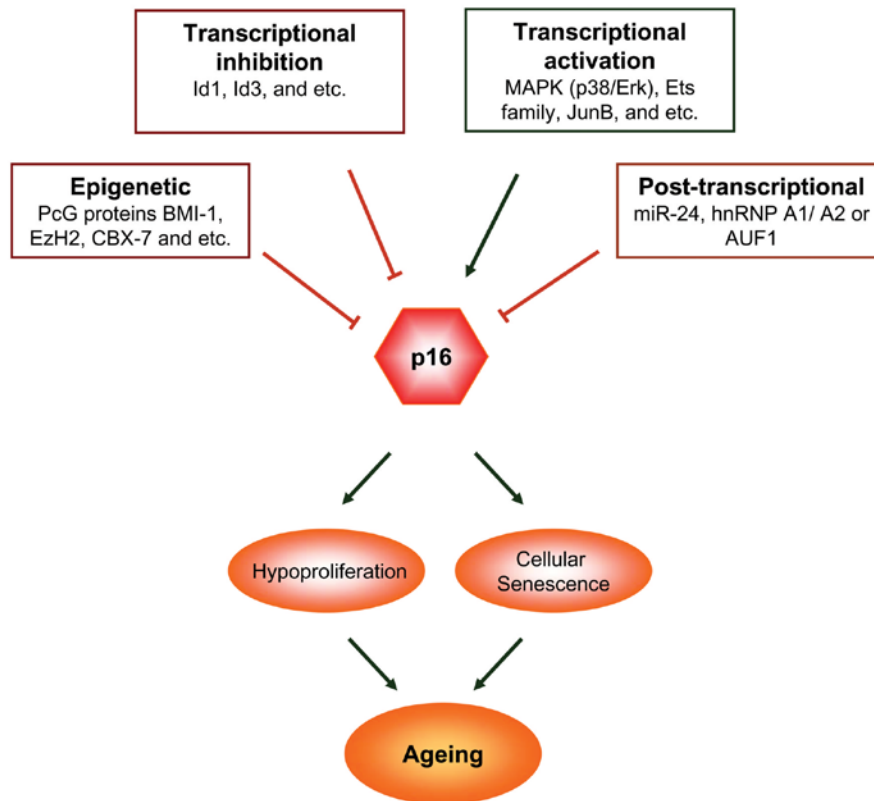


Figure 8. **Regulation of p16INK4a and its role in ageing.** Activation of p16INK4a can be achieved through a variety of mechanisms, including epigenetic, transcriptional, and posttranscriptional regulation. Once activated, p16INK4a inhibits the proliferative kinases CDK4/6, leading to immune ageing through induction of hypo-proliferation, and perhaps cellular senescence [108].

AIMS OF THE PROJECTS

PROJECT 1

Isolation and characterization of Satellite Cells (SCs) from patients affected by Amyotrophic Lateral Sclerosis (ALS)

ALS is an adult onset neurodegenerative disease defined as a progressive muscular paralysis reflecting degeneration of MNs in the primary motor cortex, brainstem and spinal cord [66]. Recently, it has been shown skeletal muscle tissue seems to play a role in ALS pathogenesis in conjunction with other cell types Dobrowolny [68]. The connection between skeletal muscle and motor neurons (MN) is crucial for both cell types in order to function throughout the life. Skeletal muscle possess the remarkable ability to regenerate after damage. This property relies on the presence of Satellite Cells (SCs), a population of adult muscle stem cells. However, the muscle regenerative capacity declines with aging and in several neuro-muscular pathological conditions. Nowadays, it is still unrevealed if loss of skeletal muscle strength and function in ALS can be due also to potential alteration in the activity of SCs and their myogenic. In this work, we isolated and characterized SCs from patients affected by ALS. A morphological and molecular study was conducted in order to understand and define possible alteration in the regenerative property of SCs in a neuromuscular disease such as ALS.

PROJECT 2:

The role of P16^{Ink4a} in skeletal muscle regeneration

The cell cycle regulator P16^{Ink4a} has been studied as an important tumor suppressor functioning as mediator of cellular senescence to prevent malignant progression of tumor cells [109]. Its expression has been shown to increase with age in several mammalian tissue [92]. Recently, P16^{Ink4a} has been involved in the reduction of regenerative capacity of different stem cell compartment during aging. Aged mice lacking P16^{Ink4a} display improved regenerative capacity [94, 97-98]. However, the role of P16^{Ink4a} in adult myogenesis has never been investigated. In this study we will use two P16^{Ink4a} knock out mouse models, a germline mutant and a conditional inducible *Pax7CreERtm;P16^{Ink4a} flox/flox*, to delete P16^{Ink4A} specifically in Pax7⁺ SCs and their downstream progeny in order to investigate P16^{Ink4a} function during repair of adult and aged muscle. Understanding the role of P16^{Ink4A} in adult SCs will lead new insight into the skeletal muscle stem cell biology. Moreover, enhancing the regenerative capacity of SCs, new therapeutic strategies can be developed for the treatment of muscle disease and aged-associated sarcopenia.

RESULTS

ALS myoblasts show a greater ability to proliferate but fail to properly differentiate

Skeletal muscle cells were isolated from muscle biopsies (*vastus lateralis*) of 7 patients affected by ALS (Age: mean $63,7 \pm 9,6$ years). However, we were able to obtain and expand skeletal pure muscle cell cultures only from 3 biopsies, independently from the disease status of patients. Indeed, we know from our previous works [110] that the quantity of muscle biopsied is critical to obtain a successful culture of pure skeletal myoblasts, while reducing contamination of other cells, such as fibroblasts. Skeletal muscle cells are characterized by the expression of a specific muscle marker. Therefore, the purity of our cultures, based on Desmin marker, was 60% (Figure 1A). Five days after isolation, all cell cultures contained rare undifferentiated mononucleated cells with rounded morphology. Then they acquired a typical elongated and spindly shape after 7 days in growing conditions (Figure 1B). At 15 days of culture, ALS myoblasts needed to be expanded and passed every 4 days at a ratio of 1 to 2, which corresponds to their doubling time. Human ALS myoblasts reduced their capacity to proliferate *in vitro* after 5 passages acquiring the typical flatted morphology of senescent cells, similar to healthy age-matched control (Ctrl) myoblasts.

The maintenance of skeletal muscle mass during life depends principally on the capacity of SCs to be activated and initiate the myogenic program, in order to differentiate and repair muscle damage [14]. Therefore, we first analyzed the proliferative ability of ALS myoblast cultures. The growth curve showed a significant proliferative advantage of ALS myoblasts after 8 and 12 days of culture ($P < 0,05$; $P < 0.0001$) (Figure 2A) compared to Ctrl. In addition, the analysis of the Ki67, a cellular marker for proliferation, confirmed that ALS

myoblasts are characterized by increased proliferation activity after 4, 8 and 12 days of culture (Figure 2B, C) compared to Ctrl, as shown from the quantification of Ki67⁺ cells (P<0.0001) (Figure 2B). Our results demonstrated that myoblasts isolated from ALS patients rapidly proliferate *in vitro*. Next, we asked if ALS myoblasts were also able to progress through the myogenic program and differentiate *in vitro*, forming multinucleated myotubes. In order to differentiate, ALS and Ctrl myoblasts were cultured in low serum media (DM), for 7 days and stained for Myosin Heavy Chain (MHC), marker of differentiated myotubes. When ALS myoblasts were switched to low-mitogen media, they began to elongate and form thin myotubes with few myonuclei (Fig. 2D). After 7 days in DM, fusion index, calculated as the ratio of the number of myonuclei fused into myotubes on the total number of nuclei and expressed in percentage, was significantly lower in ALS compared to Ctrl myoblasts (P<0.001) (Figure 2D).

Thereby, ALS myoblasts show a high capacity to proliferate *in vitro*. Nonetheless, their differentiative potential seems to be compromised. Indeed, they do not progress properly through the myogenic program, giving rise to defective myotubes formation.

Proliferating ALS myoblasts show ultrastructural feature of high undifferentiated cell and cellular abnormalities during differentiation

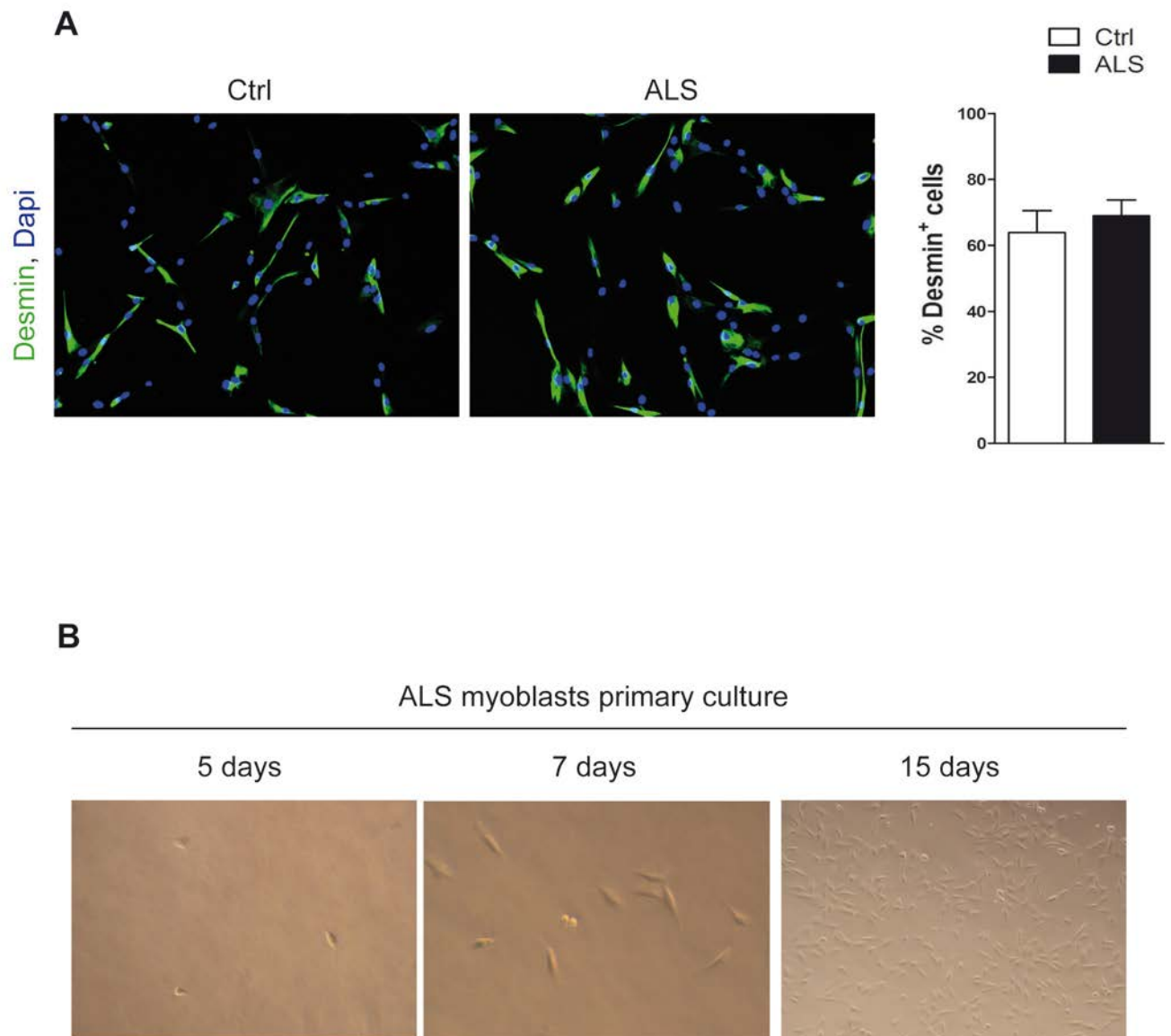
Transmission Electron Microscopy (TEM) analysis was carried out to evaluate the ultrastructural features of ALS myoblasts *in vitro* during proliferating and differentiating conditions. ALS myoblasts cultured in proliferating media showed a very immature and undifferentiated morphology compared to Ctrl myoblasts. ALS myoblasts were characterized by a tangled mass of rudimentary myofibrils and only few SR (Sarcoplasmic Reticulum) (Figure 3B, D) compared to Ctrl (Figure 3A, C). In addition, no mitochondrial ultrastructural abnormalities were detected (Figure 3D). Upon differentiation

ALS muscle cells revealed the presence of two different cell populations. Indeed, ALS myogenic cells showed differentiative elements, such as a large number of organized myofibrils with a prominent electron dense Z-line and SR with a parallel alignment (Figure 4B, D) as the Ctrl differentiated muscle cells (Figure 4A, C). Among ALS cells, we also observed some differentiated muscle cell with degenerative features. In particular, these cells were characterized by the presence of pyknotic nuclei and areas containing few degenerating vacuoles and no myofibrils (Figure 4E, F).

Our experimental analysis suggested that the partial deficiency of ALS myoblasts to differentiate may be due in part to some degenerative mechanisms, such as necrotic or apoptotic process.

Changes in MRFs expression reflect ALS myoblasts high proliferation and defective differentiation potential

Skeletal muscle SCs are regulated by MRFs, which are indispensable for progression through the myogenic program [14]. In order to investigate whether change in MRFs expression are involved in defective myogenesis of ALS myoblasts, we analyzed transcript and protein levels of Pax7, MyoD, Myf4 (Myogenin), MHC by real time qRT-PCR and Western Blot. Our results revealed an increased expression of MyoD transcript and protein and reduced transcript level of Pax7 during proliferation in ALS myoblasts compared to Ctrl, suggesting that proliferating ALS myoblasts are in a more committed phase (Figure 5A, B). Upon differentiation, MyoD expression was reduced and Myf4 remains at low expression level in ALS myoblasts (Figure 5A, B). Of note, low transcript levels of MHC were observed in ALS myoblasts compared to the Ctrl (Figure 5A), confirming the low expression of MHC protein in the smaller ALS myotubes (Figure 2D). Therefore, ALS myoblasts show alteration in the myogenic regulation which reflects their inability to properly differentiate.

FIGURES**Figure 1****Figure 1. Primary ALS myoblasts cell culture.**

A. The purity of primary ALS and healthy aged matched control (Ctrl) myoblast cell cultures was quantified based on Desmin expression. Myoblasts were stained for Desmin (green) and Dapi (blue). Magnification: 20x.

B. Bright field images of freshly isolated ALS myoblasts after 5, 7 and 15 days in culture. Magnification: 20x, 10x.

Data presented as mean and SD.

Figure 2

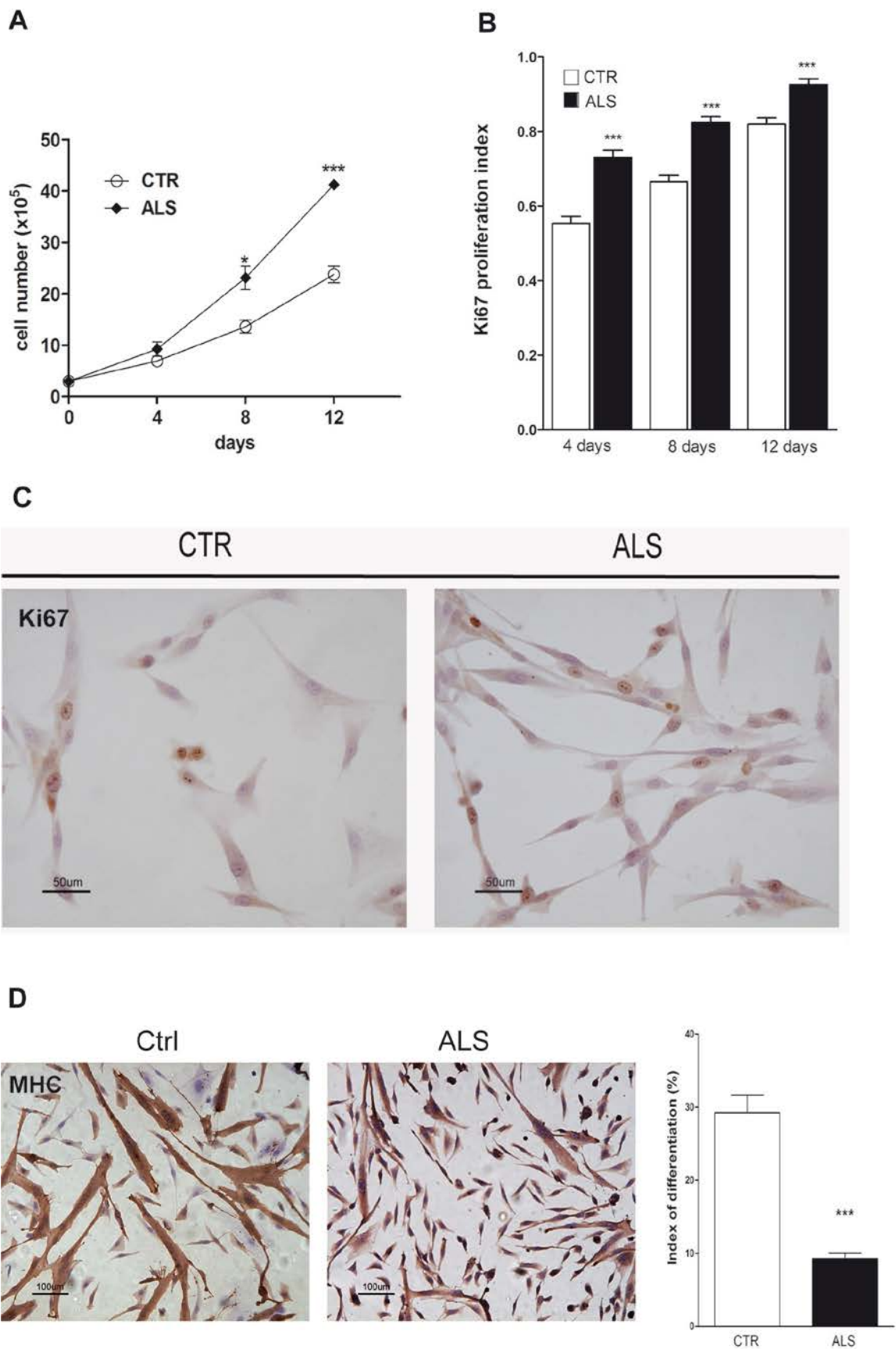


Figure 2. ALS myoblasts show a greater ability to proliferate but fail to properly differentiate

A. Growth curve of primary ALS and Ctrl myoblast cultures. The total number of cell after 4, 8 and 12 days in culture was plotted relative to the initial cell number at 0 day (n=3).

B. Quantification of Ki67⁺ proliferating ALS and Ctrl myoblasts after 4, 8 and 12 days in culture (n=3).

C. Representative immunohistochemistry staining for Ki67 proliferation marker in ALS and Ctrl primary myoblast cultures. Scale bars represents 50µm.

D. Primary myoblasts from ALS and Ctrl were switched to differentiating media (DM) for 7 days and stained for MHC. Index of differentiation was calculated.

Data presented as mean and SD (p<0.05)

Figure 3

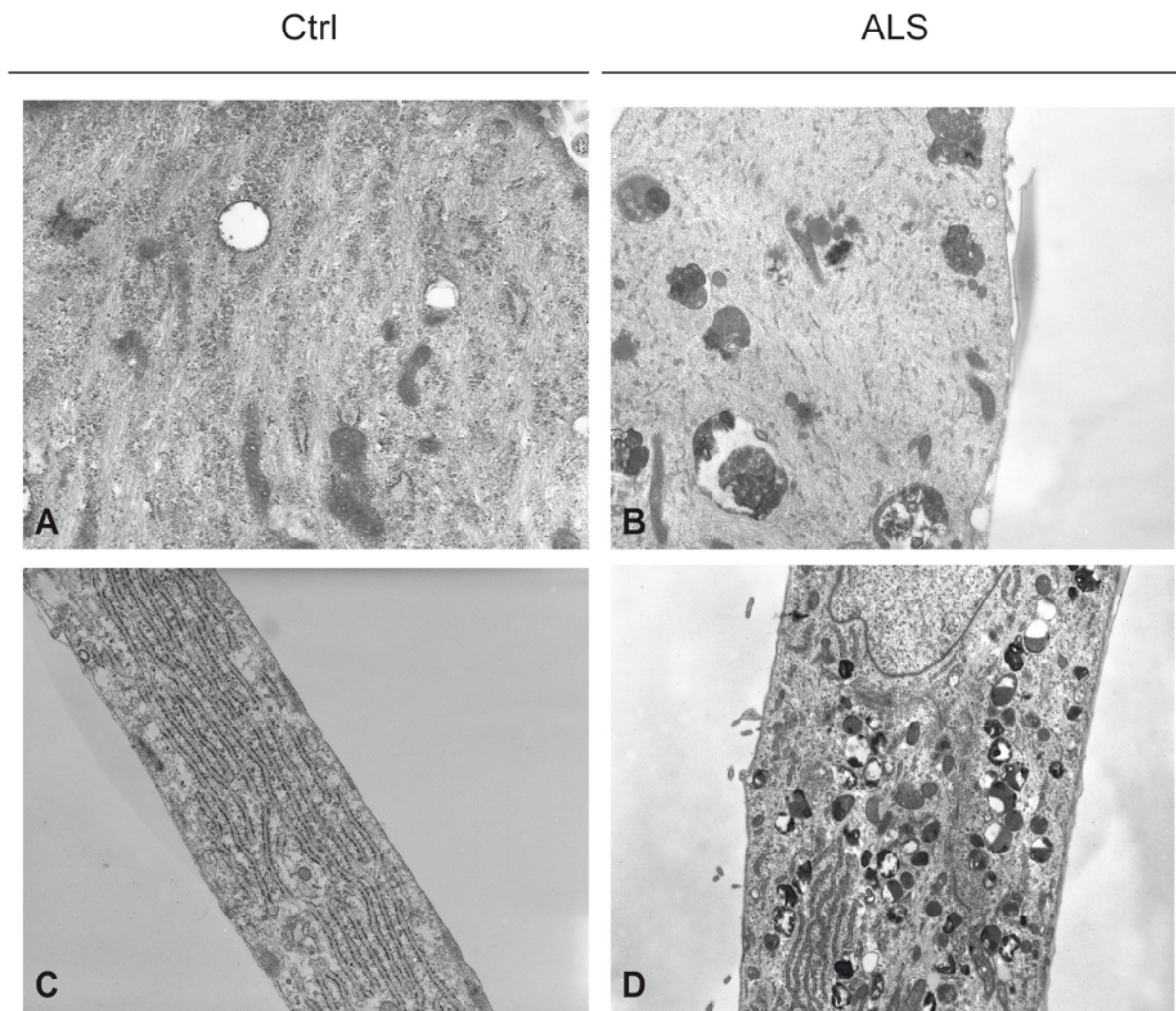


Figure 3 Proliferating ALS myoblasts show ultrastructural feature of high undifferentiated cells

TEM analysis was performed in proliferating Ctrl (A, C) and ALS (B, D) primary myoblasts. Magnification: A, B x28.000, C, D x36.000

Figure 4

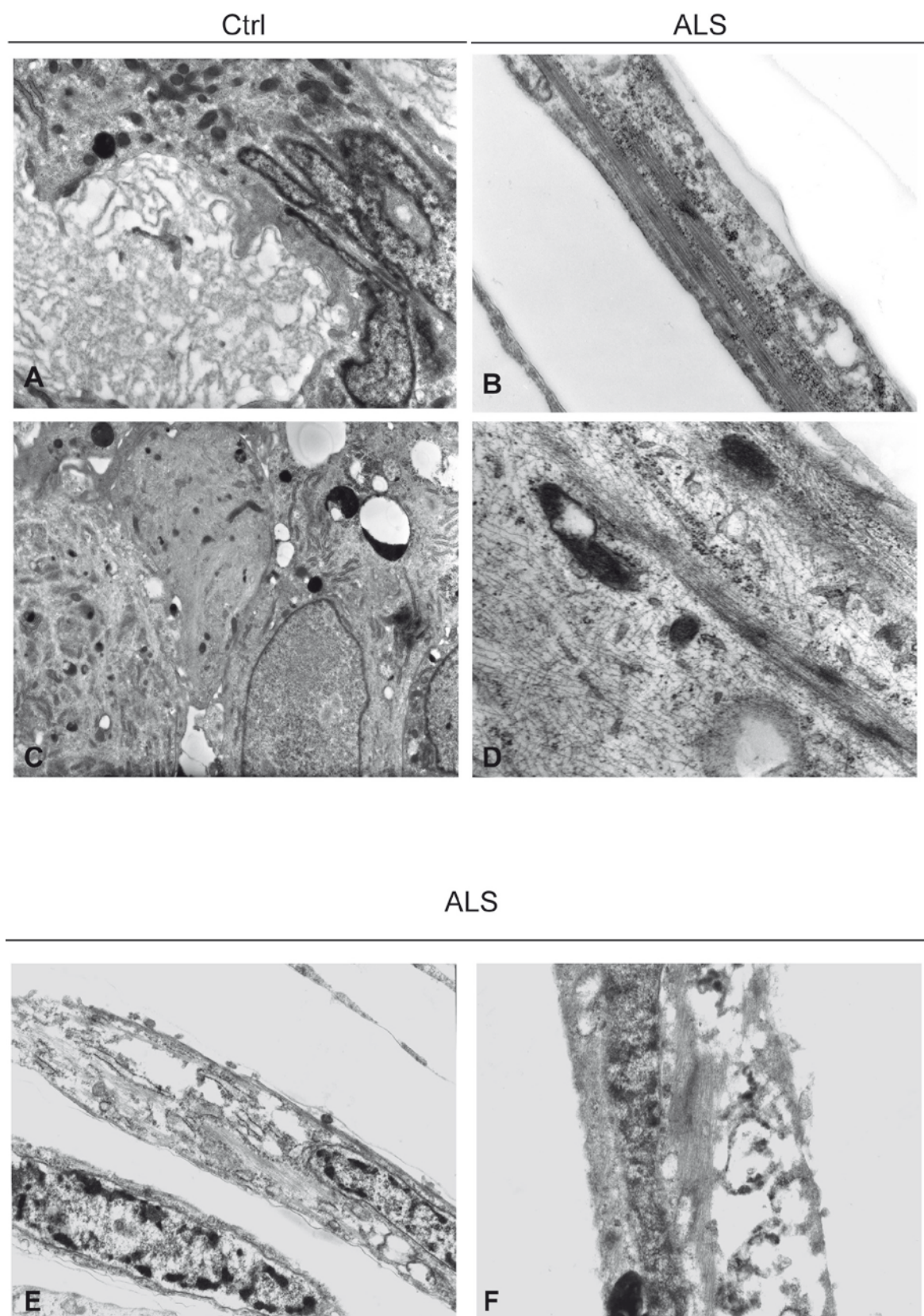
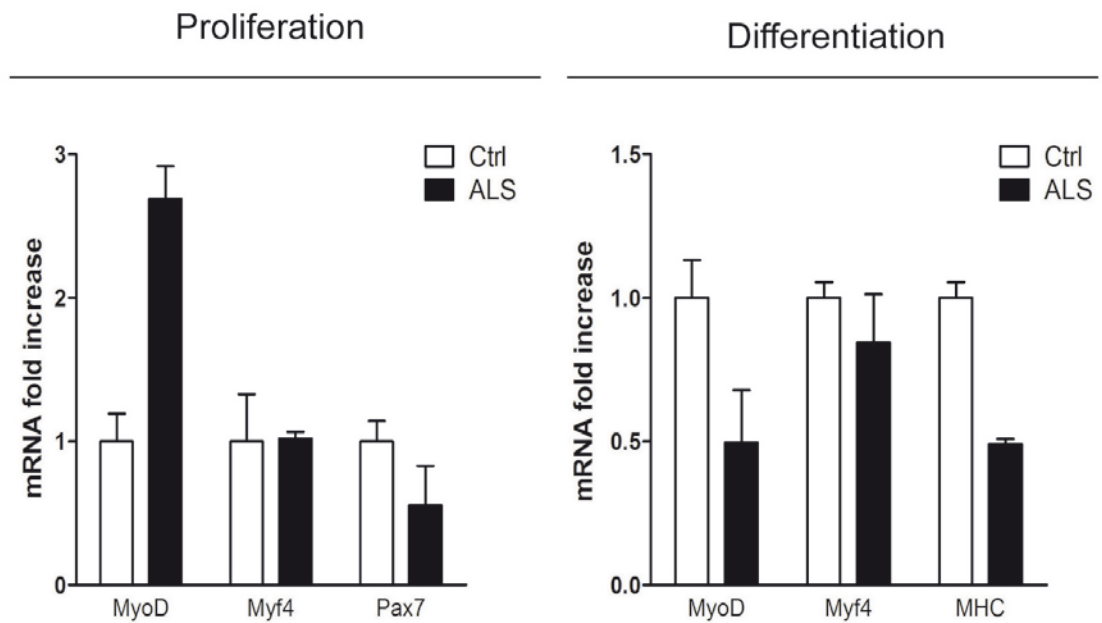


Figure 4. ALS myoblasts show cellular abnormalities during differentiation

TEM analysis was performed in differentiating Ctrl (A, C) and ALS (B, D, E, F) primary myoblasts. Magnification: A x5.400, B, E, F x3000, C, x9.100, D x10.000.

Figure 5

A



B

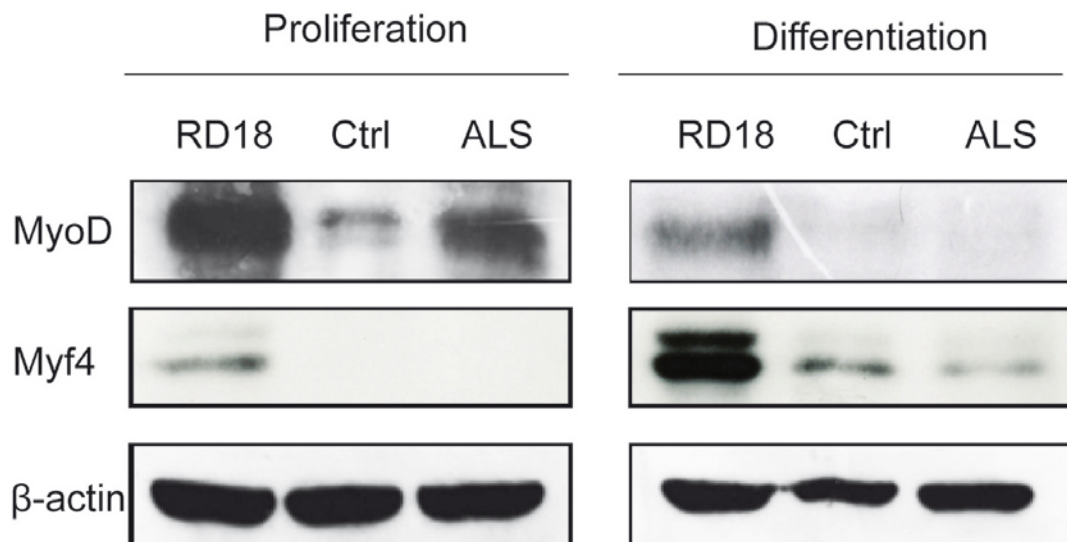


Figure 5. ALS myoblasts show changes in MRFs expression

A. MyoD, Myf4, Pax7 and MHC transcript level were assessed by real-time qRT-PCR from ALS and Ctrl primary myoblasts in proliferating and differentiating culture conditions (n=3).

B. Western Blot analysis of MyoD and Myf4 in proliferating and differentiating ALS and Ctrl myoblasts. RD18 cells (rhabdomyosarcoma cell line) were used as positive control.

DISCUSSION

Amyotrophic Lateral Sclerosis (ALS) represents one of the most common form of adult-onset Motor Neuron Diseases (MND), characterized by progressive muscle weakness caused by gradual degeneration of upper and lower motor neurons (MNs) [66]. MNs degeneration and muscle atrophy are the major pathological process associated with ALS, suggesting that nerve activity plays an extremely important role in muscle homeostasis and remodeling. However, whether muscle atrophy in ALS patients is independent from MNs degeneration or results from it remained to be defined. A direct influence of skeletal muscle tissue on pathogenesis in mouse models of ALS has recently been demonstrated [68, 76]. Nonetheless, little is known about the role of muscle Satellite Cells (SCs) in ALS patients. Therefore, in this study we wanted to understand why skeletal muscle regeneration process in patients affected by ALS results insufficient leading to severe muscle atrophy and loss of strength.

We established quite pure primary muscle cells culture ($\geq 60\%$ desmin+) from SCs isolated from 3/7 ALS patients and 3/3 aged-matched healthy control. The reason why we were not able to isolate or expand SCs from the other 4 ALS patients can be due to the small amount of human muscle biopsies, which is critical in order to obtain successful primary myoblasts cells culture [110]. Moreover, the establishment of pure muscle cell cultures in some case failed for the massive presence of other cell types, such as fibroblasts which may affected the small number of myogenic cells. The primary function of SCs is to ensure skeletal muscle maintenance, repair and regeneration [14]. Therefore, their activation, proliferation and differentiation are important process in order to preserve skeletal muscle structure and function. It remains unclear why the pool of SCs in denervated muscle does not compensate for the loss of muscle mass

during post-denervation atrophy. In our study, we observed that SCs derived from ALS patients give rise to myoblasts which possess higher capacity to proliferate *in vitro* compared to aged-matched control. These results may reflect the intrinsic character of SCs in ALS patients muscle. Indeed, SCs can be continuously activated in order to counteract skeletal muscle degeneration due to denervation leading to the exhaustion of the SCs pool. Several studies on rat model showed that denervation causes accelerated SCs activation [111], but long term denervation leads to exhaustion of the SCs pool in rat muscle [112].

In contrast to our result, Pradat et al (2011), found that human ALS myoblasts cultures showed abnormal morphological features defect in proliferation, and cellular senescence after 20 divisions [82]. This discrepancy may be related to several factors such as the disease status of patients, or different type of muscle used to isolate SCs. We did not observe any significant morphological change which was synonymous of cellular senescence in proliferating ALS myoblasts. Moreover, when we analyzed ALS myoblasts at the TEM, we noticed that, compared to aged-matched healthy control, they are still in an undifferentiated state characterized by few SR and a mass of rudimentary myofibrils.

The progression through the myogenic process is finely regulated by a complex interaction between MRFs which specifically activate the transcription of key muscle genes [32]. We found that ALS myoblasts show alteration in the control of lineage progression by MRF which can explain their incapacity to properly differentiate. The transcription profile of ALS myoblasts show that these cells are in a more committed state given that Pax7 gene expression is lower and MyoD is significantly upregulated. MyoD interacts with cell cycle regulators, in order to drive the cell proliferation towards differentiation at G1, regulating the transcription of downstream MRFs, such as Myogenin [83, 113]. Therefore, MyoD upregulation can regulate the increased proliferation of ALS myoblasts in combination with other cell cycle genes. However, the ultrastructural study of ALS myoblasts show that these cells are still more immature compared to healthy aged-matched controls. Moreover, the increased expression of MyoD does not correspond to increased Myogenin mRNA and protein level during the differentiation, as well as MHC, which is significantly

low expressed in ALS myotubes. Therefore, several molecular and pathophysiological defects may contribute to alter the molecular signature in ALS myoblasts. Indeed, the differentiation program of ALS myoblasts seems to be partly affected. We observed differentiated cells with fully formed myofibrils, SR and electron-dense Z line. However, part of differentiating ALS myoblasts seems to go through degenerative process such as apoptosis or necrosis, which can be due in part to the altered regulation of the myogenic program or ALS pathological mechanisms.

Our study shows that ALS myoblasts were able to proliferate *in vitro*, but possess defective differentiation leading to the formation of thinner myotubes, characterized in some case by degenerative aspects. The cause of these dysfunction is still unknown. Future experiment will be useful to determine whether SCs defects in ALS muscle regeneration may be considered as part of a non cell autonomous process. Therefore, we will increase the number of patients and consider also patients affected by other neuromuscular disease. Moreover, it will be interesting to study and identify growth factors or cytokines which are involved in the regulation of ALS myoblasts that can affect their capacity to growth and differentiate. All these studies, coupled with animal models, will clarify our findings.

EXPERIMENTAL PROCEDURES

SCs ISOLATION AND MYOBLASTS PRIMARY CULTURE

Samples were obtained from biopsies of vastus lateralis muscle of 7 ALS patients and 3 healthy aged-matched patients as control (Ctrl) submitted to an arthroprosthesis of the hip. The study protocol was approved by our institutional ethics committee. All patients gave their informed consent to the procedure. A small muscle tissue sample (20–370 mg) was taken without the use of electrocautery. The muscle samples were then plunged into cold (4°C) phosphate buffered saline (PBS) or Dulbecco's Modified Essential Medium (DMEM) plus 5% penicillin and streptomycin (Sigma-Aldrich, St Louis, MO, USA) and immediately transferred to the laboratory or kept at 4°C for a maximum of 48 hours before processing. The muscle samples were processed as previously described (Corbu et al, 2010). Briefly, the muscle biopsies were weighed and washed several times with M1, and then finely minced with scissors and incubated at 37°C with 5% of CO₂ with pronase (Sigma-Aldrich) (0.1% w/v) for 1 hour under gentle shaking. After the digestion step, the SCs were dissociated from the tissue by spinning for 1 minute at 950 g. The supernatant was precipitated by spinning for 5 minutes at 1500 g. The pellet was resuspended and vigorously triturated with a 10 ml pipette in DMEM plus 10% foetal bovine serum (FBS), 1% penicillin and streptomycin two or three times in order to dissociate the residual SCs in the tissue. Thereafter, the cellular suspension was left to rest for a few minutes and the supernatants were passed through a nylon filter (40µm) to remove cellular debris and processed for culturing. The cell suspension was plated in 2 cm² dishes coated with type I collagen (Sigma-Aldrich) in growing medium (GM) which is made up of Ham's F10 (Sigma-

Aldrich), DMEM (1 : 1), 15% FBS, 10% horse serum (HS) and 0.006 mg/ml basic fibroblast growth factor (bFGF) (Sigma-Aldrich) to stimulate proliferation and maintained in an incubator at 37°C with 5% CO₂. In order to look at myogenic differentiation, cells at 80-90% of confluence, were switched to a differentiating medium (DM) made up of DMEM supplemented with 2% FBS and 1% antibiotics, to allow myotubes formation. The myogenicity and the purity of the culture were determined analysing desmin expression by immunocytochemistry (clone D33, Dako, Glostrup, Denmark).

IMMUNOFLUORESCENCE AND IMMUNOCYTOCHEMISTRY

Immunofluorescence staining was performed in LabTek Chamber Slides (Nunc, Thermo Fisher Scientific) where cells had been seeded at a concentration of 3×10^3 /well. Cells were fixed with 2% Paraformaldehyde (PFA) for 10 minutes at room temperature (RT), briefly washed twice with PBS and permeabilized with 0.2% Triton X-100/PBS (PBSTx) for 5 minutes at RT. After three washes in PBS, cells were saturated for 30 min with blocking buffer (1% bovine serum albumin [BSA]) and incubated for 1 hour with primary antibody at 37°C in blocking buffer. Secondary antibody incubation was done for 1 hour at 37°C. Then cells were mounted with ProLong Gold antifade reagent with DAPI (Invitrogen; UK). Different fields for each slides were observed with a fluorescence microscope coupled with a digital camera. The fusion index was analyzed by myosin heavy chain (MHC) staining using rabbit anti-skeletal myosin (Sigma, USA, 1:10 in BSA 1% PBS), with Alexa-fluor 488/430 secondary antibody (Pierce 1:500). For immunocytochemistry analysis cells were grown on plastic coverslips of 13 mm in diameter, fixed in ice cold methanol for 10 minutes, then incubated with mouse anti-human desmin 1/200 (clone D33, Dako), mouse anti-human Ki67 1/50 (Dako) and further incubated with a rabbit EnVision anti-mouse peroxidase secondary antibody (Dako). Then cells were incubated with 3,3-diaminobenzidine (DAB) for 5 minutes,

counterstained with hematoxylin and mounted with DPX mountant for microscopy (BDH, Laboratory Supplies, Poole, UK).

ELECTRON MICROSCOPY

Cell cultures were washed with 0.01 M PBS, fixed with 2.5% glutaraldehyde in 0.1 M phosphate buffer (pH 7.4) and post-fixed with 1% osmium tetroxide in cacodylate buffer. All samples were dehydrated and detached from the plastic dish with propylene oxide, centrifuged and embedded in araldite ultrathin sections, stained with uranyl acetate and lead citrate and observed with a Philips 400T Transmission Electron Microscope.

RNA EXTRACTION AND QUANTITATIVE REAL TIME PCR

Total RNA was extracted using Trizol® reagent (Invitrogen, UK) according to the manufacturer's instructions and then reverse transcribed using an RNA polymerase chain reaction (PCR) commercial kit (MLV reverse transcriptase; Invitrogen). The procedure was conducted according to the manufacture protocol. Quantitative Real-Time PCR was performed using PowerSYBR Green PCR Master Mix (*Applied Biosystems*, USA) on ABI Prism® 7700 Sequence Detection System/Gene Amp (*Applied Biosystems*, USA). Relative levels of target genes were normalized on the expression of human beta-actin. The cycling protocol provides an initial step of 50°C for 2 minutes and 95°C for 10 minutes, followed by 40 cycles of 95°C for 15 seconds and 60°C for 1 minute. Genes expression was estimated using the relative cycle threshold (Ct) method.

Real-time PCR Primers:

Myod Fw cactacagcggcgactcc, taggcgccttcgtagcag;

Myf4 Fw cagctccctcaaccaggag, Rev gctgtgagagctgcattcg;

Mhc-1 Fw tttaaggtcgcattctctacgc, Rev aaatggccatctcagagtcg;

Pax-7 Fw cactgtgaccgaagcaactgt, Rev ctccttctgtccgcttca;

Beta-Actin Fw cctggacttcgagcaagagatg, Rev ggaaggaaggctggaagagtg

WESTERN BLOT

For Western blotting analysis cells harvested were lysed in ice-cold buffer (Tris-HCl 0,01M pH 7.6, NaCl 0,1M, Triton X-100 0,1% , EDTA 0,001M pH 8, PMSF 1 mM, DTT 1 mM 50X ,Na₃VO₄ 1 μM) supplemented with protease and phosphatase inhibitors cocktail (complete 2x , *Roche*, Italy). After 30 minutes of ice-incubation, samples were centrifuged for 15 minutes at 13,000 rpm and 4°C to remove insoluble debris. Proteins in the supernatants were quantified by Lowry assay. 50 μg of sample proteins were mixed 1:4 with Laemmli sample buffer (Tris-HCl pH 6.8 60 mM, 2% SDS, 5% glycerol, 2,5% β-mercaptoethanol and 0,01 % bromophenol blue) and heated at 95°C for 5 minutes. Protein extracts were separated by 10 % SDS-polyacrylamide gel and then transferred to nitrocellulose membranes for immunoblotting. Blots were blocked for 1hour with blocking solution (BS) (TBS-T 3% Milk 1,5% BSA) and probed with the specific primary antibodies: mouse anti-MyoD (*Dako*, USA; 1/200 in BS), mouse anti-Myogenin (*Santa Cruz Biotech*, U.S.A; 1/200 in BS) overnight at 4°C. A mouse anti-β-Actin antibody (*Santa Cruz Biotech*, U.S.A; 1:500 in BS) was used as expression control for total extracts.

STATISTICAL ANALYSIS

Experiments were performed in triplicate and means and standard deviation was calculated. A student's T test was employed to determine statistical significance. P<0.05 was considered statistically significant.

RESULTS

***P16^{Ink4a}* drives the expansion of proliferating myogenic cells both in adult and aged mice**

The regenerative ability of skeletal muscle relies on the population of Pax7⁺SCs. Following injury SCs are activated, as myoblasts, and undergo rapid proliferation starting approximately at 2 days after injury. Then, they differentiate and fuse to form new muscle fibers. A small percentage of proliferating SCs self-renew and reconstitute the SC pool [35]. The cell cycle inhibitor P16^{ink4a} has been considered as an important tumor suppressor functioning as a mediator of cellular senescence and its role has been associated with the regulation of stem/progenitor cell function in different tissue during aging [92, 94, 97-98]. Here, we characterized the expression of P16^{ink4a} in SCs and their progeny. We first examined *P16^{ink4a}* transcript level in myoblasts (MB), reserve cells (RC) and myotubes (MT) *in vitro* (Figure 1B, C). *P16^{ink4a}* transcript levels were higher in proliferating MB, compared to RC and MT. *P16^{Ink4a}* transcript correlates with protein level as shown from Western Blot analysis in MB, RC and MT (Figure 1C). P16^{ink4a} expression has been found to increase with aging in different mammalian tissue [92]. We next investigated *P16^{ink4a}* transcript levels during regeneration in adult and aged mice. *Tibialis Anterior/Extensor Digitorus Longus* (TA/EDL) muscle from adult and aged mice was injected with 50µl of 1.2% barium chloride (BaCl₂) and allowed to regenerate from 2 to 30 days. Myogenic cells were obtained by Fluorescent-Activated Cell Sorting (FACS) from uninjured and regenerating adult muscle (Figure 1A). Compared to uninjured muscle, *P16^{ink4a}* expression was significantly increased at 2 days of regeneration, when SCs are proliferating, and

then decreased as regeneration progressed, when most myogenic cells are differentiating (6, 13 days) and non-cycling (30 days). $P16^{ink4a}$ levels, as expected, were found to be slightly increased in aged myogenic cells compared to adult (Figure 1D). Therefore $P16^{ink4a}$ expression in myogenic cells is temporally regulated and correlates with proliferative phase of regeneration *in vivo*. To test the role of $P16^{ink4a}$ during myogenesis *in vitro* and *in vivo* we used $P16^{ink4a}$ knock out (P16 Null) adult and aged mice. Initially, we tested whether absence of $P16^{ink4a}$ affects SC progenitor cell proliferation. Cultured myogenic cells, obtained by FACS from adult and aged muscle, were counted and compared to adult and aged wild type (WT). In absence of $P16^{ink4a}$ adult and aged myoblasts showed increased growth rate (Figure 1E). Moreover, single fibers cultured for 48 hours and pulsed with BrdU, confirmed that loss of $P16^{ink4a}$ significantly increase the percentage of cycling transient amplifying myogenic progenitors cells (TAC) ($Pax7^+$, $BrdU^+$) both in adult and aged compared to WT adult and aged control (Figure 1F). We next asked whether the rapid expansion of P16 null myoblasts affected the generation of fusion competent myogenic cells. Myogenic cells from adult WT and P16 Null were cultured for 6 days in growing condition and then switched to low-mitogen media for 3 days. P16 Null myoblasts were able to form numerous multinucleated myotubes as the WT (Figure 1G). Together, these data suggest that $P16^{ink4a}$ expression is restricted to activated SCs and that loss of $P16^{ink4a}$ increase the proliferation of myoblasts, but does not prevent differentiation.

Loss of $P16^{ink4a}$ rescues the pool of early progenitors and defective regeneration in aged muscle

During aging there is a gradual functional decline in muscle SCs and their capacity to repair muscle [59, 114]. Pax7 is a marker of adult SCs and is required for the formation of adult SCs pool [21]. The majority of $Pax7^+/MyoD^+$ activated

TAC cells progress towards the differentiation program characterized by downregulation of Pax7 and upregulation of Myogenin [14]. Therefore, based on myogenic lineage markers, we asked whether adult and aged P16 Null myogenic progenitors were enriched for a TAC character. Single muscle fibers suspension culture from adult and aged WT and P16 Null mice were stained and analyzed for the number of Pax7⁺ and Myogenin⁺ cells, as a readout of early and late lineage respectively. Our results show a reduction of Pax7⁺ cells in aged versus adult WT. In P16 Null adult and aged muscle fibers there was an expansion of Pax7⁺ cells at expense of Myogenin⁺ cells compared to WT cultures. Significantly, in P16 Null aged fibers the pool of Pax7⁺ cells was restored to adult WT level (Figure 2A). Therefore, during aging the absence of *P16^{Ink4a}* enriches the pool of Pax7⁺ cells. To test the role of *P16^{Ink4a}* *in vivo* during skeletal muscle regeneration, TA/EDL muscles from adult and aged WT and P16 Null were injected with 50µl of 1.2% BaCl₂. Control and regenerated muscles were collected and analyzed after 6 days of regeneration. Uninjured muscles were morphologically similar between WT and P16 Null mice (data not shown). Immunohistochemical analysis of the 6 days regenerating TA revealed an increase of the number of cycling (Myod⁺/Ki67⁺) Pax7⁺ cells in absence of *P16^{Ink4a}* both in adult and aged (Figure 2B). Moreover formation of new myofibers was enhanced in adult and aged regenerating P16 null muscles compared to age matched controls. Significantly loss of *P16^{Ink4a}* function in aged muscle rescued fiber formation to levels of adult WT controls (Figure 2C). Together these results demonstrate that *P16^{Ink4a}* loss during aging increases the number of Pax7⁺ cells and rescues defect in aged myofibers formation.

SC specific *P16^{Ink4a}* inactivation alters myoblast proliferation independent of senescence

To bypass potential caveats associated with germline deletion of genes we used a *Pax7CreERtm*; *P16^{Ink4a flox/flox}* and tested the role of *P16^{Ink4a}* in Pax7⁺ SCs

[35, 115]. The $P16^{Ink4a}$ conditional allele has a floxed sites flanking exon 1 α of the *Ink4a/Arf* locus and somatic excision of $P16^{Ink4a}$ does not alter expression of $P15^{Ink4b}$ or *ARF* (Figure 3A, 5A), in contrast to germline $P16^{Ink4a}$ inactivation [115]. Deletion of $P16^{Ink4a}$ can be achieved *in vitro* with Adenovirus-Cre infection to target *loxP* sites. Myoblasts were isolated from *Pax7CreERtm*; $P16^{Ink4a\ flox/flox}$ mice and infected with Ad5CMV-eGFP (Ctrl) and Ad5CMVCre-eGFP ($P16^{f/f}$) (Figure 3A). With this approach we were able to target the $P16^{Ink4a}$ deletion in SCs progenitor *in vitro*, resulting in an approximately a 95% efficiency of infection and $P16^{Ink4a}$ deletion, based on GFP expression (Figure 3B). First, we examined if specific deletion of $P16^{Ink4a}$ in SCs progenitors affect their proliferation ability. Twenty-four hours after infection, Ctrl and $P16^{f/f}$ myoblasts were pulsed with BrdU (5 μ M) for 12 hours and analyzed at 12, 24 and 36 hours (Figure 3C). The growth curve and number of Pax7 cells that incorporate BrdU revealed that in absence of $P16^{Ink4a}$ Pax7⁺ progenitors cells maintain the capacity to proliferate more compared to Ctrl, in agreement with the $P16^{Ink4a}$ null germline model (Figure 3C, 1E). $P16^{Ink4a}$ has been implicated as mediator of cellular senescence [109]. Therefore, to test whether the proliferative advantage gained by $P16^{f/f}$ myoblasts was due to changes in cellular senescence, we performed a SA- β -galactosidase assay. Unlike a positive control for senescent embryonic stem cells, (Mouse Embryonic Fibroblasts, MEFs), Ctrl and $P16^{f/f}$ cultures were negative for SA- β -galactosidase expression (Figure 3D). Therefore, acute deletion of $P16^{Ink4a}$ specifically in SCs increased the rate of proliferating SC progenitors in absence of cellular senescence.

SC $P16^{Ink4a}$ deletion alters myogenic fate decisions

Given that loss of $P16^{Ink4a}$ increased the proliferation rate of SC progenitors we wanted to evaluate their progression through the myogenic program. In particular we expected that $P16^{f/f}$ myoblasts were enriched for a TAC (Pax7⁺/MyoD⁺). Indeed, 48 hour after adenovirus infection $P16^{f/f}$ myoblasts

showed expansion of Pax7⁺/MyoD⁺ cells with also a slight increase in the pool of reversibly quiescent Pax7⁺/MyoD⁻ cells compared to Ctrl (Figure 4A). Next, as in the *P16^{Ink4a}* knockout model, we investigate their capacity to differentiate. Twenty-four hours after adenovirus infection, Ctrl and *P16^{f/f}* myoblasts were switched to low-mitogen media and left to differentiate for 3 days. *P16^{f/f}* myoblasts were able to progress through the differentiation program, forming multinucleated myotubes (Figure 4B). These *in vitro* experiments confirm the results obtained with the *P16^{Ink4a}* knockout model. Therefore, acute deletion of *P16^{Ink4a}* in myoblasts expands the Pax7⁺/MyoD⁺ pool. Moreover, this enriched population of proliferating myoblasts is able to differentiate and fuse to form multinucleated myotubes.

SC specific *P16^{Ink4a}* inactivation affects cell cycle regulators and MRFs expression

P16^{Ink4a} activation is regulated at the transcriptional level by MAPK signaling via ERK and p38MAPK [87]. Moreover, this signaling pathway is involved in the modulation of other cell cycle regulators that may contrast and/or cooperate with *P16^{Ink4a}* activity [87]. We studied the effect of *P16^{Ink4a}* deletion on the expression of other cell cycle regulators in relation to the control of myogenic lineage progression by MRFs. We performed a Mouse MAP Kinase Signaling RT² Profiler™ PCR Array that profiled the expression of 84 genes related to the MAP Kinase signaling pathway (Figure 5A). The PCR array was done on Ctrl and *P16^{f/f}* myoblasts 18 hours after adenovirus infection. Among all the genes evaluated we focused our attention on the most significant genes related to the G1 cell cycle phase regulation. Then, we validated the array analyzing the transcript level of *P16^{Ink4a}*, *Cdkn1b* (*p27*), *Cdkn1a* (*p21*), *Ccnd1* (*Cyclin D1*) and *Cdkn1c* (*p57*) (Figure 5 B). After 18 hours recovery from Cre infection *P16^{Ink4a}* levels were reduced by ~60% compared to Ctrl. Nonetheless, partial deletion of *P16^{Ink4a}* significantly affected the expression of other cell cycle genes. *p27*, *p21*,

p57 belongs to the Cip/Kip CKIs inhibitors that specifically bind to and block the activity of CDK2 complex. However, Cip/Kip members can associate with CDK4/6 and have a stimulatory effect by promoting the assembly of the active cyclin–CDK complex [116]. *p21* and *p57*, but not *p27*, are significantly upregulated in absence of *P16^{Ink4a}*, as well as *Cyclin D1*. Next, we analyzed the MRFs transcript profile. Significantly, loss of *P16^{Ink4a}* decreases *Myf5* and *Myogenin*, upregulating *Pax7* and *MyoD* transcript level (Figure 5B). This was in accordance with the lineage progression analysis where we observed expansion of *Pax7⁺/MyoD⁺* TAC in the absence of *P16^{Ink4a}*. Therefore, these results demonstrate that *Cyclin D1* and Cip/Kip CKI cell cycle inhibitors are sensitive to *P16^{Ink4a}* deletion and are transcriptionally activated. Moreover, these changes on cell cycle gene expression are reflected in regulation of MRFs, confirming that loss of *P16^{Ink4a}* contributes to downregulate *Myogenin* and *Myf5*, promoting the expression of *Pax7* and *MyoD*.

CDK4/6 inhibition partially restores the effect of *P16^{Ink4a}* deletion

P16^{Ink4a} prevents cell cycle progression during G1 phase through its binding to CDK4/6 and inhibiting CDK4/6-mediated phosphorylation of pRB [87]. Therefore, we hypothesized that the inhibition of CDK4/6 should rescue the effect caused by *P16^{Ink4a}* deletion in SC progenitors. After adenovirus infection, myoblasts from Ctrl and *P16^{f/f}* were incubated for 18 hours with Cdk4/6 inhibitor (5 μ M) and then collected for mRNA and protein analysis (Figure 6A). Ablation of *P16^{Ink4a}* resulted in ~90% loss of *P16^{Ink4a}* protein (Figure 6B, C). Cdk4/6 rescued the expression of *p21*, *p57* and *Cyclin D1*, but it did not affect *P16^{Ink4a}*, which seemed to be independent from the CDK4/6 inhibition. Of note, *p27* was upregulated when CDK4/6 was added both in Ctrl and in *P16^{f/f}* myoblasts (Figure B, C). We also analyzed MRFs expression after CDK4/6 inhibition. In Ctrl myoblasts inhibition of CDK4/6 caused a block of cell cycle, given that all MRFs were downregulated. However, CDK4/6 did not rescue MRFs transcript and protein level in absence of *P16^{Ink4a}* (Figure B, C). Therefore, the effects of *P16^{Ink4a}* loss on cell cycle genes regulation are rapidly rescued by CDK4/6,

confirming that $P16^{Ink4a}$ acts through the CDK4/6/Cyclin D1 pathway. However, MRFs regulation is controlled by CDK4/6 and other independent mechanisms.

SC specific deletion of $P16^{Ink4a}$ enhanced progenitor expansion

To directly test the role of $P16^{Ink4a}$ in Pax7⁺ SCs and their progeny *in vivo*, we used the $Pax7Cre$ $ER^{tm};P16^{Ink4a\ flox/flox}$ mouse model ($P16^{f/f}$) to permanently disrupt $P16^{Ink4a}$ function in adult Pax7⁺ SCs upon tamoxifen (TM) administration [35, 117] (Figure 7A). $Pax7Cre$ $ER^{tm};P16^{Ink4a\ flox/flox}$ mice treated with TM were used as controls (Ctrl). It has previously been demonstrated that Pax7Cre allele or TM treatment at the dosages used in these studies do not affect SC function and muscle regeneration [35]. In the present studies, four days after TM administration, single fibers were isolated from Ctrl and $P16^{f/f}$ adult mice and cultured for 0, 2 and 3 days. Using Pax7 and Myogenin as lineage markers, we investigated if loss of $P16^{Ink4a}$ modifies the proportion of myogenic progenitors at an early (Pax7⁺/Myogenin⁻) versus late (Pax7⁻/Myogenin⁺) stage of lineage progression. We observed in $P16^{f/f}$ mice that the number of Pax7⁺ cells along single muscle fibers gradually increased and was significantly higher than the Ctrl after 3 days of suspension culture (Figure 7B, C), without any significant change in Myogenin⁺ cells number, as observed in the $P16^{Ink4a}$ knockout model (Figure 7D). Therefore, these results show that acute $P16^{Ink4a}$ deletion in SCs results in a greater expansion of the pool of early progenitor Pax7⁺ cells.

Bmi1-GFP⁺ correlates with the expansion of Pax7⁺ SCs

Bmi1 gene belongs to the PcG family and is a component of the polycomb repressive complex 1 (PRC1) that is implicated in the stable maintenance of gene repression [118]. Bmi1 has been reported to epigenetically silence the *Ink4a/ARF/Ink4b* locus [119-120]. Additionally, extensive analysis reported that Bmi1 is essential for the maintenance of normal adult HSC and leukemia stem cells as well as adult NSC [103-104, 121]. We used targeted reporter mice in

which the endogenous Bmi1 gene was replaced through homologous recombination with GFP [122] as an alternative approach to dissect the role of $P16^{Ink4a}$ in muscle SCs. Myogenic cells were FACS sorted from adult Bmi1-GFP mice based on their GFP expression. We first examined the proliferative capacity of Bmi1-GFP⁺ (High) and Bmi1-GFP⁻ (Low) myogenic cells. Bmi1-GFP⁺ myogenic cells showed increased growth rate after 7 days in culture, which is maintained also after serial plating. On the contrary, Bmi1-GFP⁻ myogenic cells stopped growing after serial plating. Given that Bmi1 suppress $P16^{Ink4a}$, Bmi1-GFP⁺ ($P16^{Ink4a}$ low) showed increased proliferation as in $P16^{Ink4a}$ knock out and $Pax7CreER^{tm}; P16^{Ink4a flox/flox}$ mice models. Bmi1-GFP⁻ ($P16^{Ink4a}$ high) may stop cycling because they start to differentiate or becoming senescent. Bmi1-GFP⁺ marks stem or progenitors cells in non-hematopoietic tissues [122]. Thus, we analyzed Bmi1-GFP and Pax7 expression on single fibers isolated from adult mice and cultured for 48 hours. Our results showed that Pax7 expression correlated with Bmi1-GFP⁺ and that the number of Pax7⁺/Bmi1-GFP⁺ increased after 48 hours, but not Pax7⁺/Bmi1-GFP⁻ cells, which remained Bmi1-GFP⁻. Therefore, these finding confirm that Bmi-1 controls $P16^{Ink4a}$ expression. Indeed, Bmi1-GFP⁺ regulates the expansion and probably the self-renewal of Pax7⁺ SCs, possibly by restricting $P16^{Ink4a}$. Moreover, Bmi1-GFP represents a very interesting model to study distinct subpopulation of SCs with differential Bmi1/ $P16^{Ink4a}$ expression both in postnatal muscle growth and adult muscle regeneration.

FIGURES

Figure 1

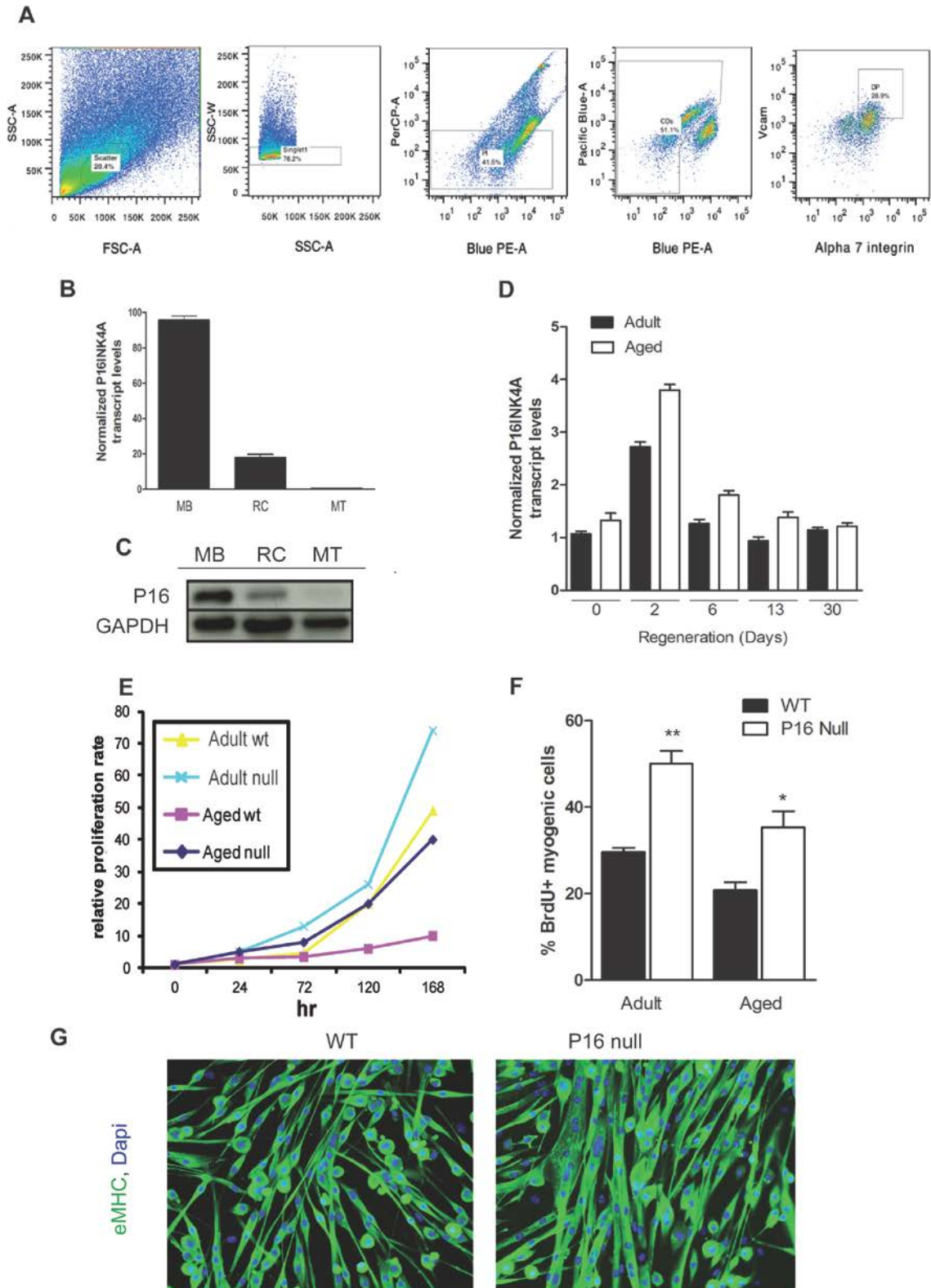


Figure 1. Loss of *P16^{Ink4a}* increases the proliferation rate of both adult and aged myoblasts without affecting their differentiation program

A. Representative FACS plots of mononucleated cells isolated from TA/EDL muscles and stained with propidium iodide (PI), anti-streptavidin VCAM biotinylated (APC), anti- α 7-Integrin (Pacific Blue), anti-CD31/45 (PE) antibodies. Double positive DP cells gated on $\text{vcam}^+/\alpha 7\text{integrin}^+/\text{CD31}^-/\text{CD45}^-/\text{PI}$ were collected and used for further study of myogenic cells.

B, C. Transcript and protein level of *P16^{Ink4a}* expression were assessed respectively by real-time qRT-PCR and Western Blot in myoblasts (MB), reserve cells (RC) and differentiated myotubes (MT) derived from FACS sorted SCs-myogenic cells cultures.

D. *P16^{Ink4a}* transcript level was assessed by real-time qRT-PCR from FACS-purified myogenic cells isolated from uninjured and regenerating TA/EDL muscle of adult and aged mice after 2, 6, 13 and 30 days.

E. Growth curve of purified myoblasts isolated from *P16^{Ink4a}* WT and Null adult and aged mice. The total number of cells after 24, 72, 120, 168 hours in culture was plotted relative to the initial cell number at 0 hour (n = 3).

F. The percentage of BrdU⁺ myogenic cells in single fibers isolated from *P16^{Ink4a}* WT and Null adult and aged BrdU-treated mice after 48 hours of culture.

G. Primary myoblasts from *P16^{Ink4a}* WT and Null adult mice were switched to low-mitogen media for 3 days and stained for eMHC (green) in order to assess their capacity to differentiate *in vitro*.

Experiments done in triplicate. Data presented as mean and SEM, n = 4-6 mice (p < 0.05).

Figure 2

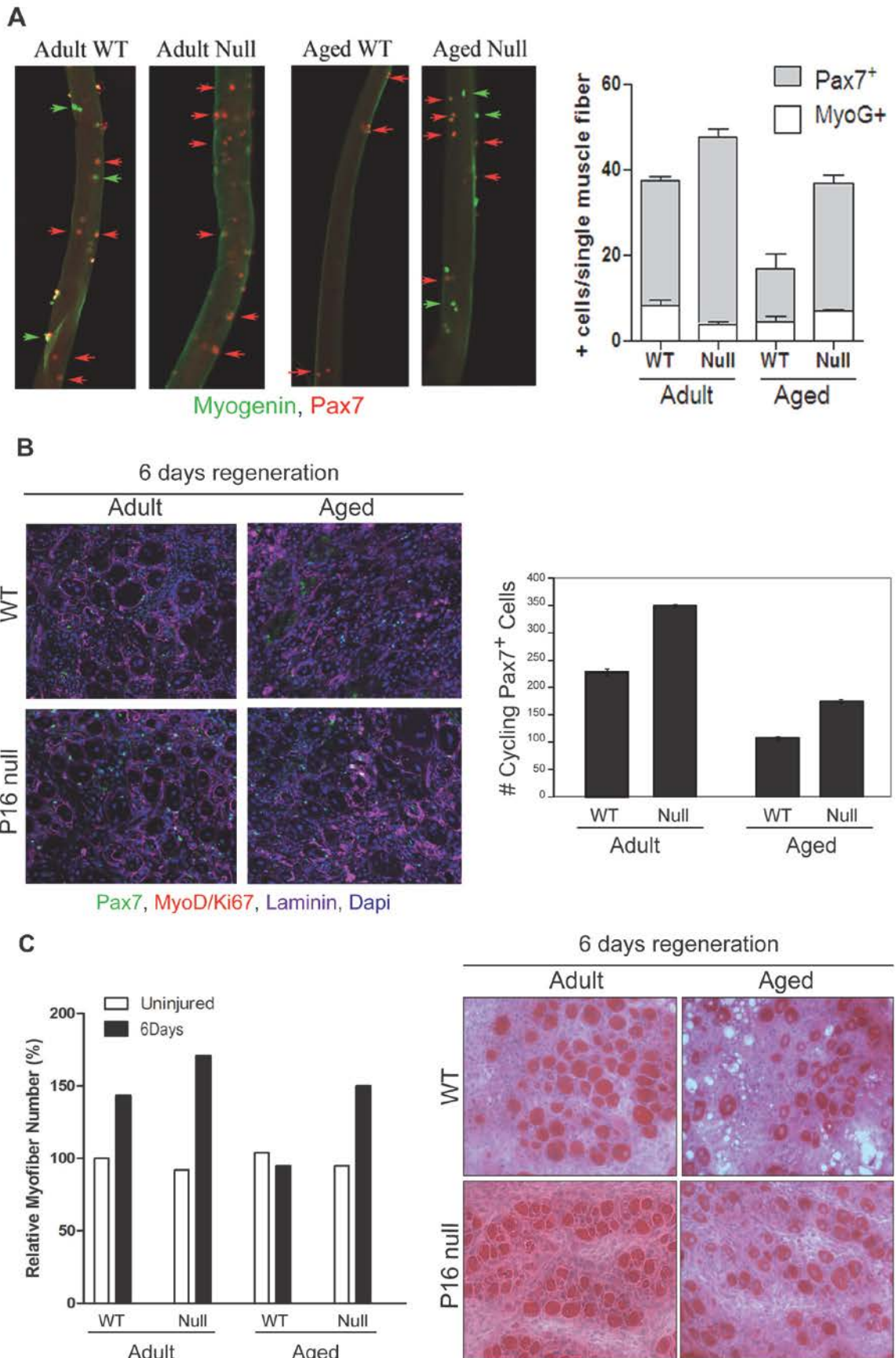


Figure 2. Absence of *P16Ink4a* restores the pool of early progenitors in aged muscle and rescues defect in aged myofibers formation.

A. Single fibers, isolated from *P16^{Ink4a}* WT and Null adult and aged mice, were cultured for 3 days and stained and quantified for Pax7 (red) and Myogenin (green) positive cells per single muscle fiber.

B. Transverse sections of regenerating TA muscle from *P16^{Ink4a}* WT and Null adult and aged mice, were stained for cycling (MyoD⁺, Ki67⁺, red) Pax7⁺ cells (green) located in sublaminar position (laminin⁺; magenta). Quantification of the total number of cycling Pax7⁺ cells per muscle section (left).

C. H&E staining of transverse section of regenerating *P16^{Ink4a}* WT and Null, adult and aged TA muscle and quantitative analysis of myofiber number expressed in percentage (%), normalized to uninjured control muscle.

Data presented as mean and SEM, n = 4-6 mice.

Figure 3

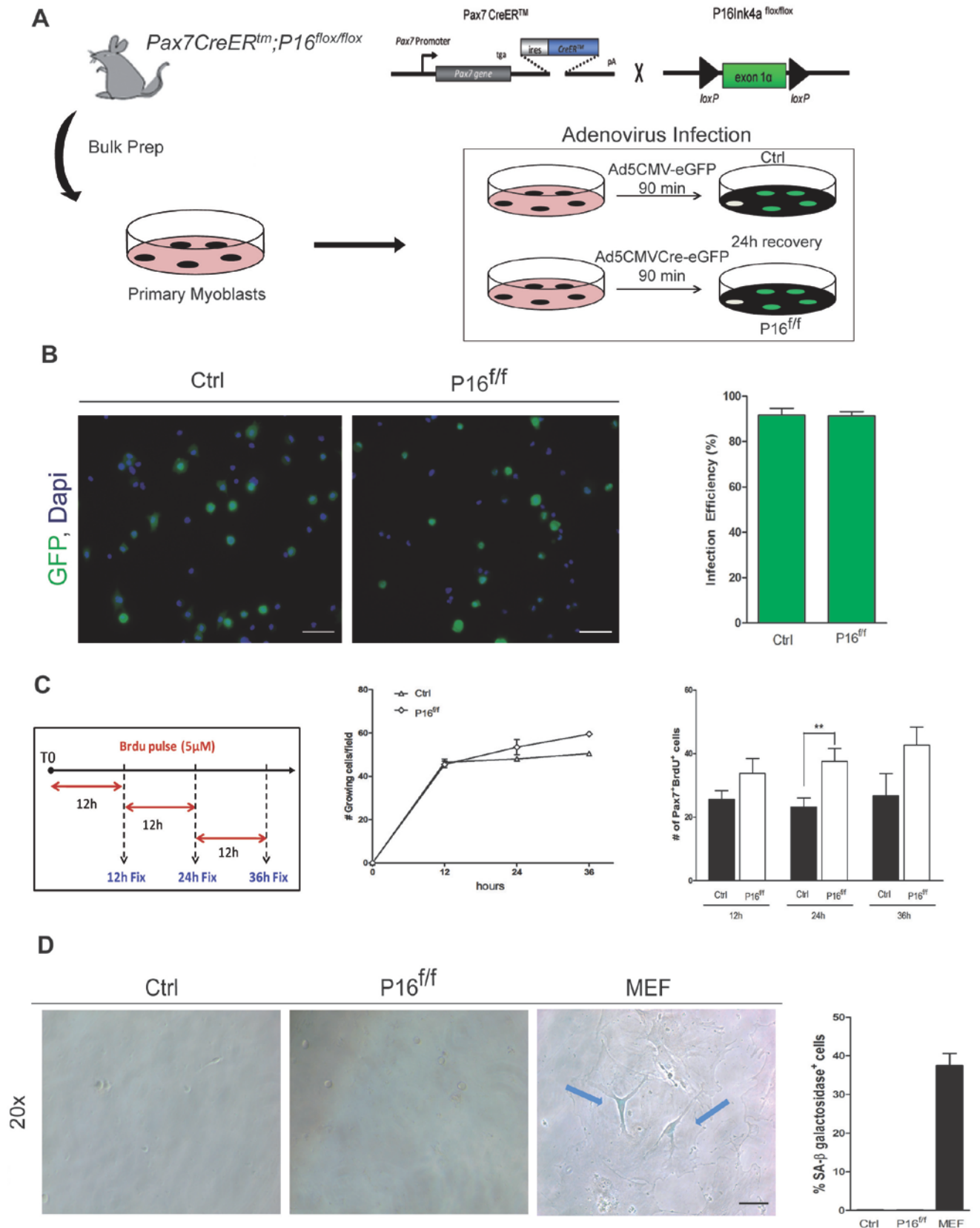


Figure 3. *In vitro* specific SCs *P16Ink4a* inactivation results in increased myoblasts proliferation rate which occurs in absence of cellular senescence.

A. Cartoon depicting the adenovirus infection strategy to induce Cre recombination activity in myoblasts obtained from *Pax7-CreERtm;P16^{flox/flox}* adult mice.

B. Representative images of *Pax7-CreERtm;P16^{flox/flox}* myoblasts infected with Ad5CMV-eGFP control (Ctrl) and Ad5CMVCre-eGFP (*P16^{f/f}*) (GFP, green). Efficiency of infection based on GFP expression expressed as a percentage (%) (left).

C. Growth curve of Ad5CMV-eGFP control (Ctrl) and Ad5CMVCre-eGFP (*P16^{f/f}*) infected myoblasts from *Pax7-CreERtm;P16^{flox/flox}* adult mice pulsed with Brdu (5 μ M) in PM for 12 hours and fixed at 12, 24 and 36 hours (cartoon). The total number of growing cells per field and the number of Pax7⁺/Brdu⁺ cells after 12, 24, 36 hours was quantified.

D. Bright field images and quantification of infected myoblasts from Ad5CMV-eGFP control (Ctrl) and Ad5CMVCre-eGFP (*P16^{f/f}*) infected myoblasts from *Pax7-CreERtm;P16^{flox/flox}* adult mice stained for SA- β -galactosidase. Serial passaged Mouse Embryonic Fibroblasts (MEFs) cultures were used as positive control. Blue arrows indicate SA- SA- β -galactosidase⁺ cells.

Data are presented as mean \pm SEM, n = 3, p < 0.05. Scale Bars represents 50 μ m.

Figure 4

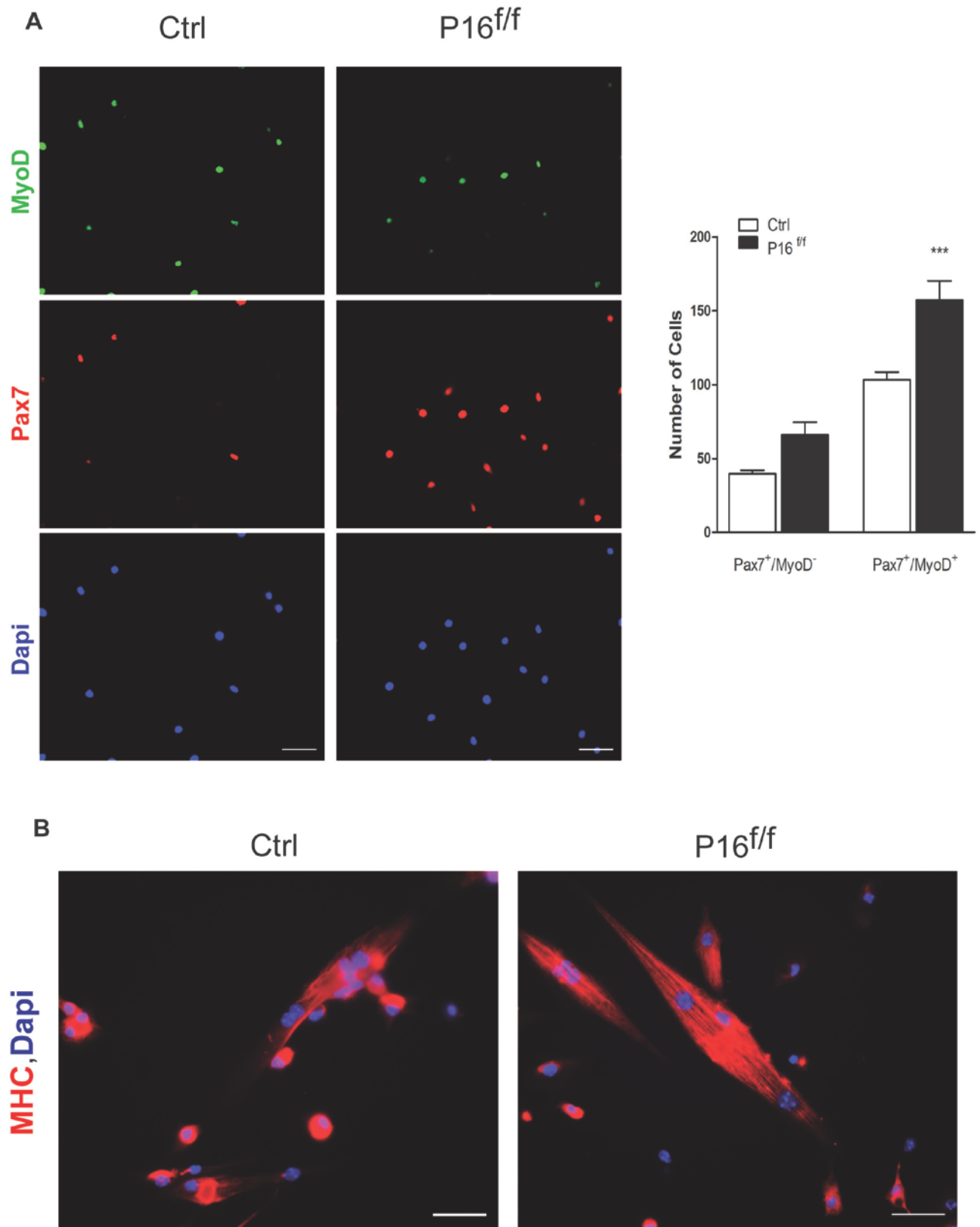


Figure 4. *In vitro* SC-specific *P16Ink4a* inactivation results in the expansion of the fusion competent Pax7⁺MyoD⁺ progenitors pool.

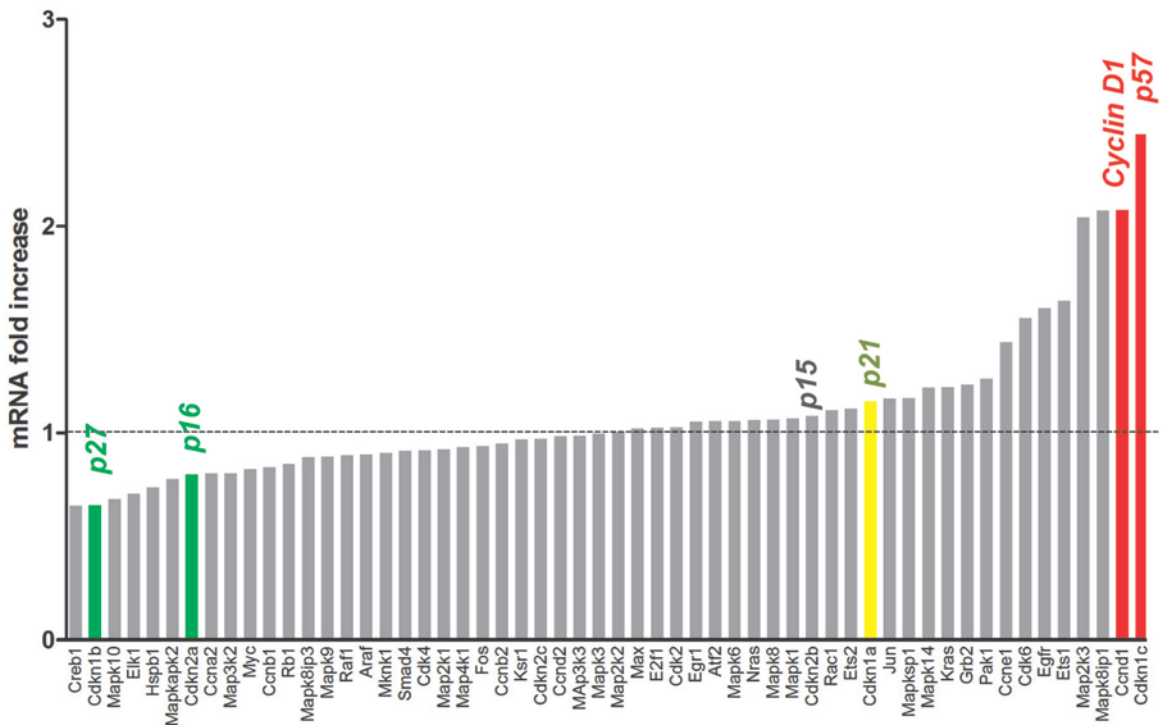
A. After 24 hours Ad5CMV-eGFP control (Ctrl) and Ad5CMVCre-eGFP (P16^{f/f}) infected myoblasts from *Pax7-CreERtm*; *P16^{flox/flox}* adult mice were stained for Pax7 (red), MyoD (white), Dapi (blue). Pax7⁺MyoD⁻ and Pax7⁺/MyoD⁺ cells were quantified as mean of 10 independent microscope fields (Pax7⁺MyoD⁻, red arrows; Pax7⁺MyoD⁺ yellow arrows; Pax7⁻MyoD⁺, green arrows)

B. Ad5CMV-eGFP control (Ctrl) and Ad5CMVCre-eGFP (P16^{f/f}) infected myoblasts from *Pax7-CreERtm*; *P16^{flox/flox}* adult mice were switched after 48h in growing condition to low-mitogen media and their capacity to fuse was assessed by MHC staining (red).

Data presented as mean ± SEM; n = 3; p < 0.05. Scale bar represents 50 μm.

Figure 5

A



B

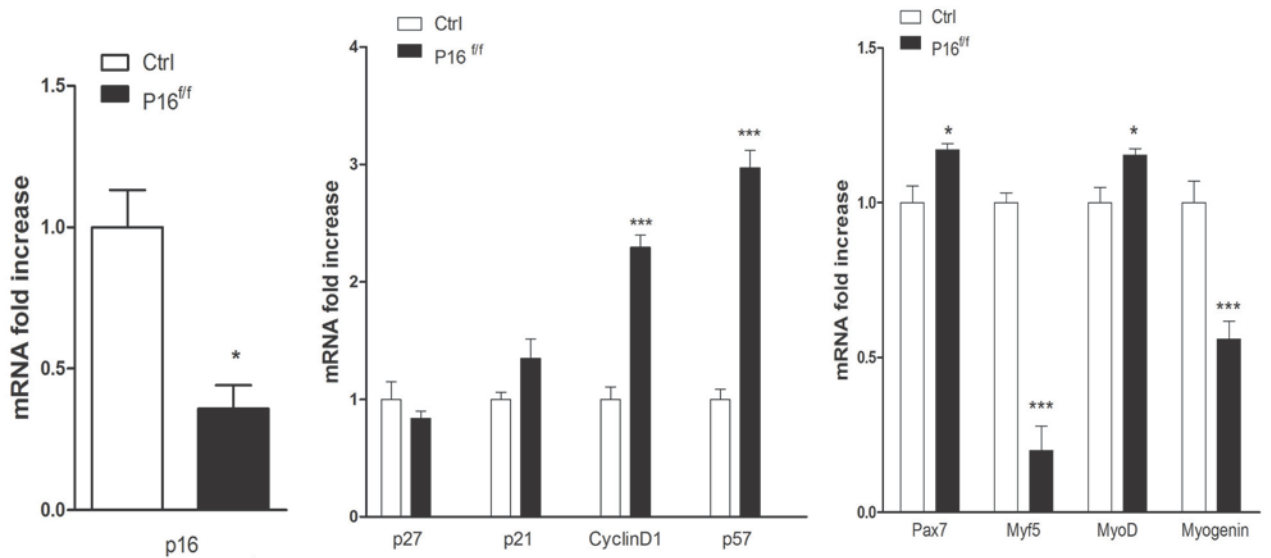


Figure 5. Effect of loss of P16Ink4a in Pax7⁺ progenitors cells on cell cycle gene regulators and MRFs

A. Gene expression analysis of Ad5CMV-eGFP control (Ctrl) and Ad5CMVCre-eGFP (P16^{f/f}) infected myoblasts from *Pax7-CreERtm;P16^{lox/lox}* mice was examined with a PCR-array focused on the MAP Kinase signaling pathway. Putative targets of P16^{Ink4a} are highlighted: *Cdkn1c* (*p57*) (red), *Ccnd1* (*CyclinD1*) (red), *Cdkn1a* (*p21*) (yellow), *Cdkn2a* (*p16*) (green), *Cdkn1b* (*p27*) (green).

Data presented as mean of value obtained from a duplicate experiment.

B. Transcript levels of *p16*, *p27*, *p21*, *p57*, *CyclinD1*, *Pax7*, *Myf5*, *MyoD* and *Myogenin* were validated by real-time qRT-PCR from Ad5CMV-eGFP control (Ctrl) and Ad5CMVCre-eGFP (P16^{f/f}) infected myoblasts isolated from *Pax7-CreERtm;P16^{lox/lox}* mice.

Data presented as mean ± SEM, n = 3, p <0.05.

Figure 6

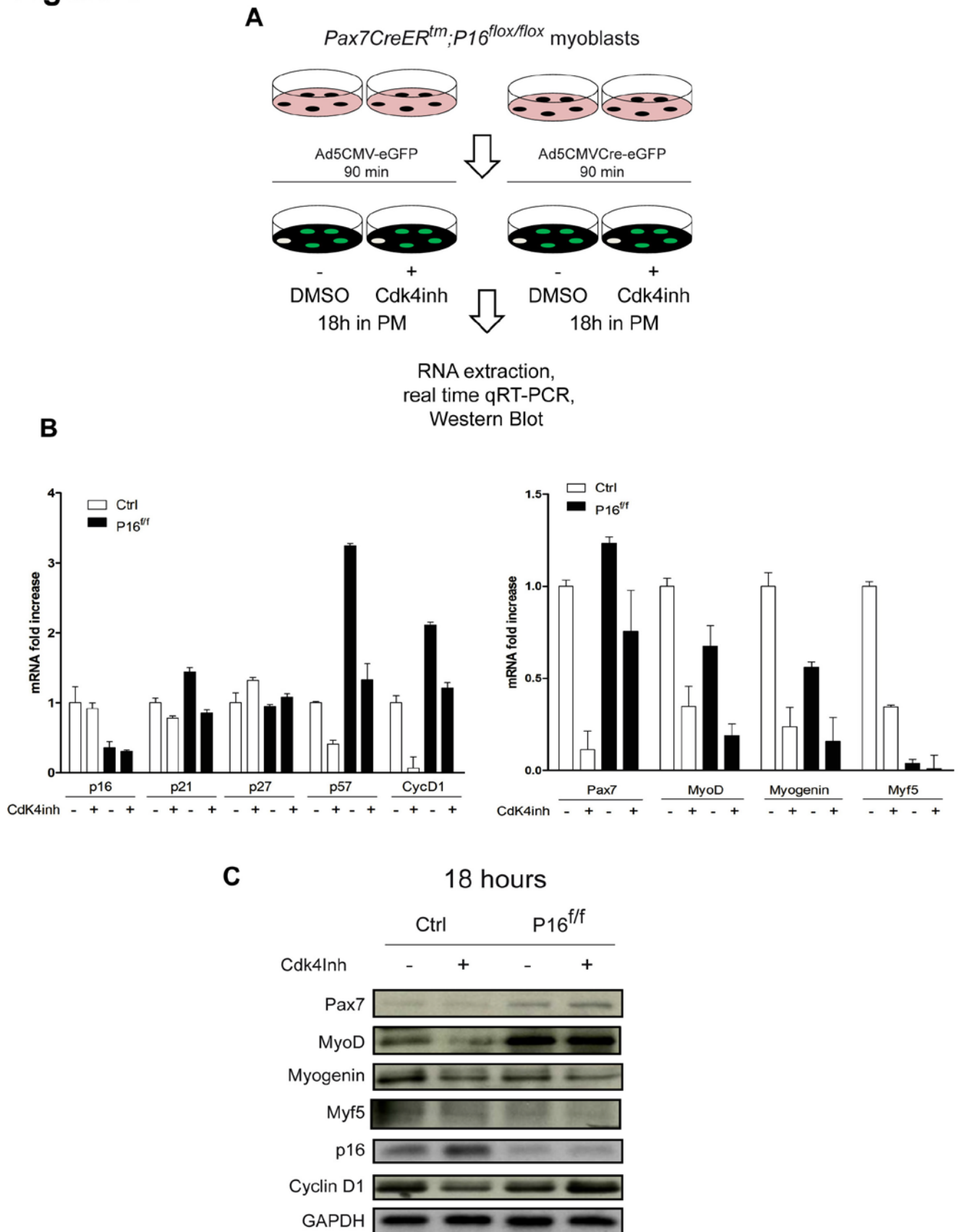


Figure 6. P16^{Ink4a} inactivation effects are partially restored by Cdk4 inhibitor, confirming the P16^{Ink4a} downstream regulation.

A. Cartoon depicting the experimental design of adenovirus infection strategy to induce Cre recombination in myoblasts obtained from *Pax7-CreERtm;P16^{lox/lox}* adult mice.

B. Transcript levels of *p16*, *p21*, *p27*, *CyclinD1*, *p57* (right) and *Pax7*, *Myf5*, *MyoD*, *Myogenin* (left) from Ctrl and P16^{f/f} myoblasts treated with Cre and Cdk4 inhibitor were assessed by real-time qRT-PCR.

C. Protein level of Pax7, Myf5, MyoD, Myogenin, p16 and CyclinD1 were analyzed by Western Blot 18 hours after Cre and Cdk4 inhibitor treatment.

Data presented as mean ± SEM; n = 3; p < 0.05.

Figure 7

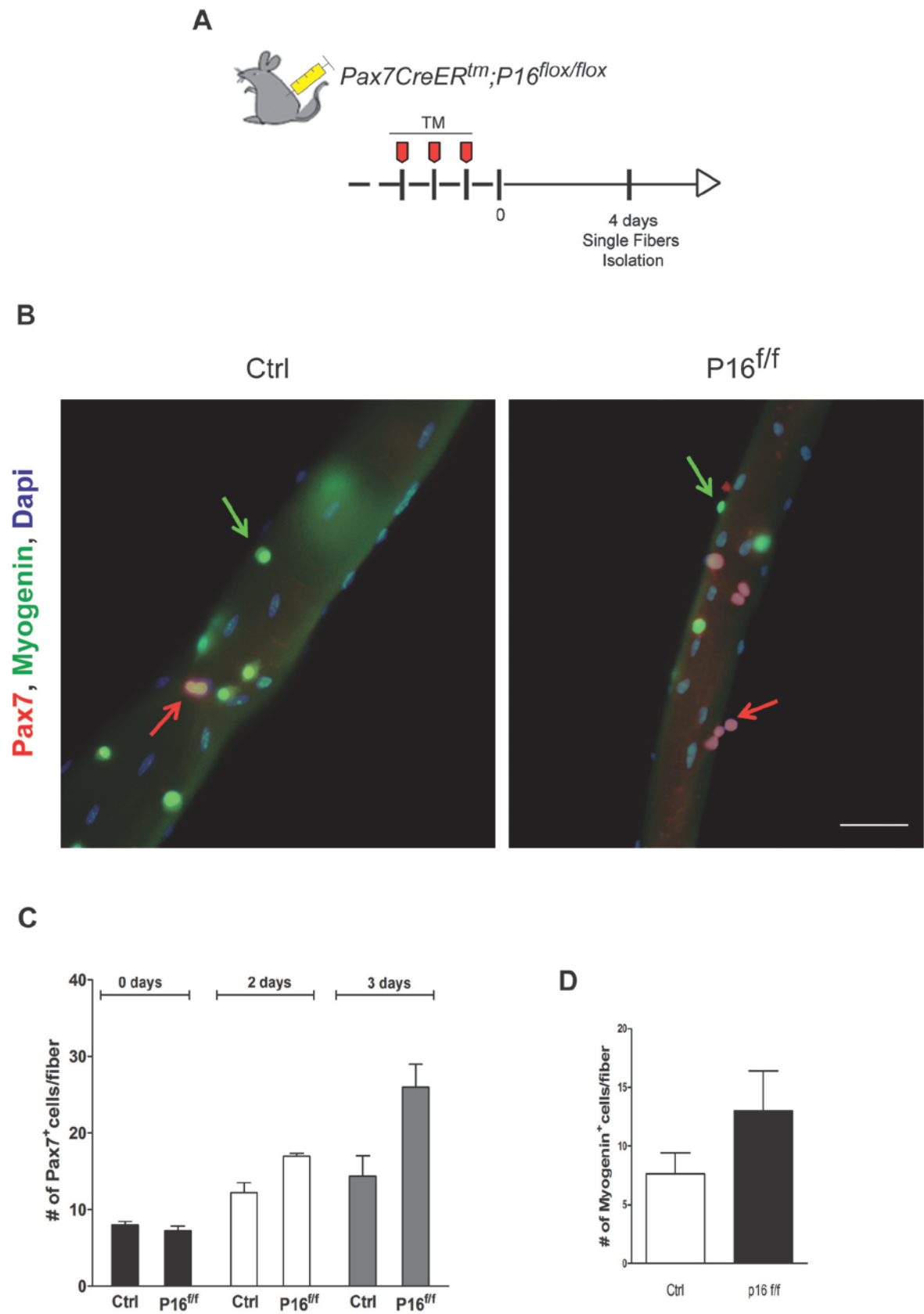


Figure 7. P16^{Ink4a} deletion from SCs *in vivo* increases the pool of progenitors cells without affecting myogenic progression.

A. Cartoon depicting the tamoxifen (TM) injection scheme for P16^{Ink4a} deletion in Pax7-Cre^{ERTm}/P16^{flox/flox}.

B, C, D. Single fibers isolated from Pax7-Cre^{ERTm}/P16^{wt/wt} (Ctrl) and Pax7-Cre^{ERTm}/P16^{flox/flox} (P16^{f/f}), were cultured in suspension for 0, 2 and 3 days and stained and quantified for Pax7 (red) and Myogenin (green) positive cells .

Data presented as mean \pm SEM; n = 3; p < 0.05.

Figure 8

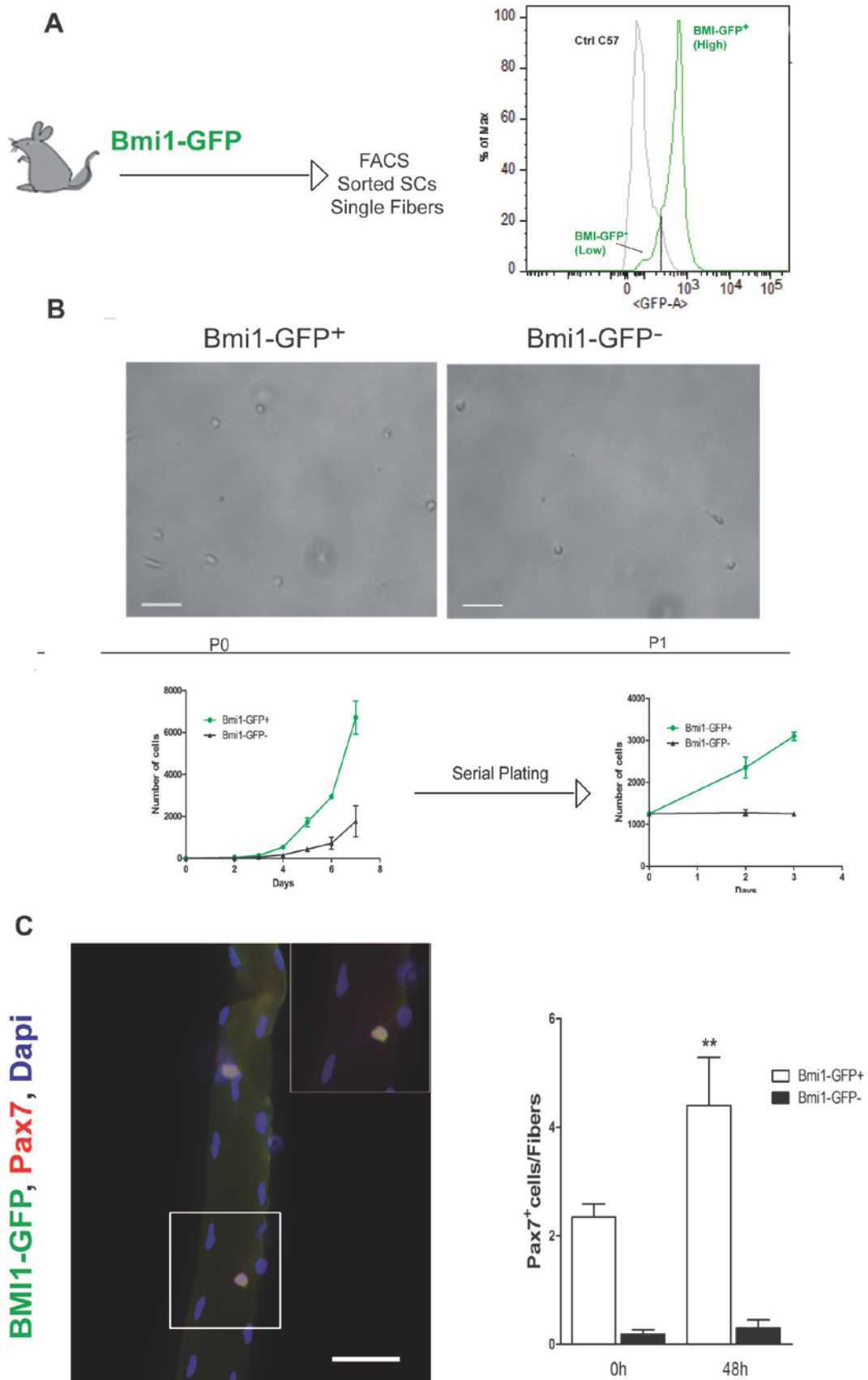


Figure 8. Bmi1-GFP⁺ correlates with the expansion of Pax7⁺ SCs

A. FACS sorted myogenic cells from Bmi1-GFP adult mice based on the GFP expression.

B. Bright field images of cultured Bmi1-GFP⁺ and Bmi1-GFP⁻ FACS sorted myogenic cells from adult Bmi1-GFP mice. Growth curve of Bmi1-GFP⁺ and Bmi1-GFP⁻ FACS sorted myogenic cells at P0 and P1 passages. The total number of cells was plotted relative to the initial cell number at 0 day.

C. Single fibers isolated from Bmi1-GFP adult mice were cultured for 0 and 48 hours and stained and quantified for Bmi1-GFP (green) and Pax7 (red) positive cells per single fiber.

Data presented as mean \pm SEM; n = 3; p < 0.05. Scale bar represents 50 μ m.

DISCUSSION

P16^{Ink4a} represents one of the most important CKIs during G1 cell cycle progression. Acting as a tumor suppressor gene, P16^{Ink4a} inhibits cell cycle preventing uncontrolled cancer cells proliferation and inducing cellular senescence [123]. Its expression rises with age in many tissues, correlated with the accumulation of dysfunctional senescent cells [124-125]. Recently, P16^{Ink4a} has been involved in the decline of the replicative capacity of different stem cell compartments, such as HSCs, NSCs and pancreatic β -cells [94, 97-98]. How P16^{Ink4a} promotes aging, limiting proliferation and self-renewal, remains still unclear and more studies are necessary to clarify if it happens through increase of senescence, block of cell cycle or other mechanisms. The role of P16^{Ink4a} in skeletal muscle stem cell biology has never been investigated. Our work highlights a novel role of P16^{Ink4a} in adult skeletal muscle stem cells, a role that is independent of senescence or aging. In the present study, we demonstrated that P16^{Ink4a} is expressed in activated and proliferating satellite cells (SCs). Whether P16^{Ink4a} expression is confined to a particular subpopulation of myogenic cells or it is expressed at low levels by all cells, it is still not clear. After damage, Pax7⁺SCs are rapidly activated to initiate the myogenic program, differentiate and eventually, form new muscle fibers and replenish the pool of SCs [35]. We found that P16^{Ink4a} expression is temporally regulated during in vivo regeneration and correlates with the activation of SCs after 2 days of regeneration and confirmed in proliferating myoblasts. Then its expression declines as soon as myogenic cells differentiate or go back to quiescence. These data probably reflects that P16^{Ink4a} can be activated by signals and growth factors that also regulate activation and proliferation of SCs, such as members of FGF family or

Notch signaling pathway [14, 52]. These signals may converge and interact with members of the MAP Kinase signaling pathway, which is involved in cell cycle regulation and it is often associated with the induction of P16^{Ink4a} [126]. Future studies can clarify and define extrinsic signals that modulate the SCs niche and therefore, regulate their activity and the regulation of P16^{Ink4a}.

In this study we used different approaches to define the role of P16^{Ink4a} in skeletal muscle SCs progenitors. In particular, we analyzed the effect of P16^{Ink4a} germline inactivation during skeletal muscle regeneration. However, in knockout mice, the inactivation of a gene can be compensated by other developmental mechanisms, such as the increased expression of other cell cycle inhibitors, for example, P15^{Ink4b} [115]. Therefore, we developed a temporally inducible, cell-specific gene deletion approach to directly target P16^{Ink4a} expression in Pax7⁺SCs and their progeny [115, 117]. Germline inactivation of P16^{Ink4a} results in increased myogenic cells proliferation. In *Pax7CreERtm;P16^{Ink4aflox/flox}* conditional knockout mice acute deletion of P16^{Ink4a} in Pax7⁺SCs progenitors increases proliferation rate. In addition, previous reports demonstrated that the number and proliferative capacity of HSCs and NSCs is increased in P16^{Ink4a} null mice [94, 97]. These findings are consistent with the role of P16^{Ink4a} as a cell cycle inhibitor. Indeed, reduced level of P16^{Ink4a} results in downregulation of *Myf5* and *Myogenin* and increased expression of *CyclinD1* in Pax7⁺SCs progenitors, without any significant compensatory increase in other CKIs except *P57^{Kip2}*. *P57^{KIP2}* participates in myogenesis [127], it stabilizes MyoD protein, through inhibition of cyclin E-CDK2 complex [128] and in turn, MyoD up-regulates *P57^{Kip2}* in a p73-dependent manner [129]. This suggests that there is a fine balance and cooperation between MRFs and cell cycle genes.

Our results suggest that P16^{Ink4a} controls early myogenic progenitors expansion in absence of cellular senescence. This change in proliferation reflects changes in SC lineage progression. Thus, P16^{Ink4a} control the lineage progression, regulating the expansion of early progenitor cells. We believe from our data that the pool of Pax7⁺/MyoD⁺ progenitor cells possesses the potential to progress through the lineage program. The temporal coordination between proliferating

progenitor cells and differentiation is a complex process regulated by multiple factors. Notch signaling pathway is required for the activation of SCs in order to form rapid cycling TAC progeny [52]. This stage is followed by a coordinated increase in Wnt signaling and decreases in Notch signaling, which drives the onset of differentiation [54]. Therefore, P16^{Ink4a} can control the expansion of early progenitors cells and the balance between extrinsic signaling pathways may finely modulate its role.

Dividing SCs progenitors can generate daughter cells with a more self-renewal and/or more committed character. Cell fate decision is critical and is regulated by symmetric and/or asymmetric cell division mechanisms. However, very little is known about SCs asymmetric division mechanisms[130-131]. From our data, P16^{Ink4a} seems to not affect the pool of self-renewal Pax7⁺SCs, but it only increases the Pax7⁺MyoD⁺ TACs compartment. During *in vivo* muscle regeneration loss of P16^{Ink4a} expands the Pax7⁺SCs early progenitors pool and increases the number of newly-formed myofibers after 6 days of regeneration. Therefore, we can only hypothesize a possible role of P16^{Ink4a} in controlling asymmetric fate decisions, but this assumption needs more studies. Future *in vitro* experiments (i.e. time lapse microscopy) will contribute to understand the role of P16^{Ink4a} during cell division and give new insight into SCs fate decision mechanism. In addition, secondary injury *in vivo* experiments will be performed in order to confirm that the increase of early progenitors in absence of P16^{Ink4a} does not affect self-renewal of the SC pool. Consistent with previous work on the P16^{Ink4a} function during aging [94, 97], we demonstrated that P16^{Ink4a} controls the expansion of Pax7⁺SCs pool in adult mice and more interesting its deletion restores the pool of early progenitors in aged mice which display improved regenerative capacity. Indeed, the decline in muscle tissue regeneration with aging is largely due to a decreased function of Pax7⁺SCs [132]. Not only, SCs activity can be affected by signals change in the aged microenvironment ([114, 132]). However, deletion of P16^{Ink4a} increases the number of cycling Pax7⁺SCs during regeneration in aged mice and enhances the formation of new myofibers, rescuing defective aged myogenesis. Moreover, activation of P16^{Ink4a} has been reported to be responsive to extrinsic signals in old mice, such as TGFβ/pSmad3.

Activation of Notch signaling pathway blocks TGF β /pSmad3 dependant upregulation of P16^{Ink4a} and restores SCs regenerative capacity [133]. Therefore, P16^{Ink4a} function in SCs during aging can be influenced by multiple extrinsic and intrinsic factors.

Consistent with the idea that P16^{Ink4a} drives cell cycle exit through pRb hypophosphorylation mediated by CDK4/CyclinD, we asked whether inhibition of CDK4 activity would rescue signaling events induced by loss of P16^{Ink4a}. Some cell cycle regulators such as p21, p57 and Cyclin D1 are sensitive to P16^{Ink4a} deletion and their transcript levels are rapidly restored after inhibition of CDK4/6. However, the regulation of MRFs seems to respond only in part to the CDK4/6 inhibition, suggesting that their regulation is not only dependent on the cell cycle state via CDK4, but many other factors can affect the expression of MRFs such as epigenetic [134-135] and post-transcriptional mechanisms [135].

Cell cycle exit and differentiation are controlled by multiple cell cycle regulators. In particular, CKIs as well as pRb family proteins play an important role in regulating differentiation [136]. However, we showed that during myogenic differentiation P16^{Ink4a} is not required for terminal differentiation. In spite of a reduction in Myogenin⁺ cells in proliferating cultures, when P16^{Ink4a} null cells are cultured under low serum conditions, they form myotubes normally, suggesting that P16^{Ink4a} is not required for terminal differentiation. Indeed, a substantial amount of literature indicates that other CKIs belonging to Cip/Kip family cell cycle inhibitors drive cell differentiation. In particular p21^{Cip} has been involved in the regulation of myogenic differentiation and p21^{Cip} null mice show impaired adult regeneration [137]. However, myogenic differentiation is also dependent on pRb family proteins. Indeed, lack of pRb in myoblasts cause severe defect of myogenesis and terminal differentiation, while proliferation is transiently enhanced [89]. Recently, it has been reported, that in Pax7^{Cre^{ER}};Rb1 conditional mice, the Pax7⁺SCs pool is expanded, but myogenic differentiation is impaired resulting in delayed muscle regeneration *in vivo* [90]. This work supports in part our observations. Nonetheless, we found that P16^{Ink4a} is not involved in myogenic differentiation, which seems to be in contrast with pRb findings. However, Kotake et al, (2007) showed that pRb family proteins are

required for recruitment of PRC2 (Polycomb Repression Complexes) to trimethylate P16^{Ink4a} promoter, priming the Bmi-1 containing PRC1L ubiquitin ligase complex to silence P16^{Ink4a} [138]. In this context our data from Bmi1-GFP mice model supports a role for P16^{Ink4a} in myogenic lineage progression. Using Bmi1-GFP knock-in mice model [122], we were able indirectly to dissect the role of P16^{Ink4a}, based on the Bmi1-GFP expression. Indeed, SCs derived from Bmi1-GFP⁺ showed enhanced proliferation of Pax7⁺SCs pool compared to Bmi1-GFP⁻ SCs. This result is consistent with the role of Bmi1 to silence P16^{Ink4a} [105]. However, P16^{Ink4a} expression in SCs progenitors can be epigenetically controlled also by other PcG. Juan et al (2011) demonstrated that Ezh2 controls self-renewal of SCs possibly through silencing P16^{Ink4a} expression [102]. It would be interesting to determine whether P16^{Ink4a} is differentially expressed in subsets of SCs that are enriched for Bmi1-GFP expression.

In conclusion, this study emphasizes a novel role of P16^{Ink4a} in Pax7⁺SCs and their progenitors during adult regeneration. Therefore, we believe that P16^{Ink4a} in SCs is not only a regulator of cellular senescence promoting aging, but it plays an important role in the regulation of SCs progenitors. Future transplant studies in injured and mouse models of muscular dystrophy will also address whether targeting P16^{Ink4a} may provide a functionally superior SC pool to enhance skeletal muscle regeneration. These findings can contribute to develop new alternative strategies to enhance SCs function in muscle aging or disease.

EXPERIMENTAL PROCEDURES

ANIMALS

$P16^{Ink4a}$ knockout mice and mice carrying the $P16^{Ink4a}$ gene flanked by a pair of *loxP* sites ($P16^{lox}$) were kindly provided by Norman E. Sharpless [115]. Mice with two copies of $P16^{lox}$ were crossed with $Pax7-CreER^{tm}$; $P16^{lox/lox}$ mice [117] to generate $Pax7-CreER^{tm+};P16^{Ink4a/lox/lox}$ (Satellite cell-specific $P16^{Ink4a}$ [$P16^{f/f}$]) and $Pax7-CreER^{tm-};P16^{Ink4a/lox/lox}$ control littermate (Ctrl). Bmi1-GFP knock-in mice were kindly provided by David T. Scadden [122]. Adult mice are 3-4 months old and aged mice are 18 months old. Animals were housed and handled in accordance with the guidelines of the MGH subcommittee for animal research.

MUSCLE INJURY

Injury to whole TA/EDL muscle from one leg was made by injection of barium chloride ($BaCl_2$) (50 μ l, 1.2%) into 30 sites in the lower limb and left to regenerate as indicated in results. The other leg remained uninjured as control.

MYOGENIC CELL PREPARATION

Single fiber cultures

Single fiber cultures: EDL muscle was digested in 0.2 % Collagenase type I (Invitrogen) in DMEM at 37°C and single fibers were gently triturated. Then, Single fibers were carefully transferred into 10 ml of 5% Horse Serum (HS) in DMEM (Dulbecco's Modified Eagle Medium, Gibco) and incubated at 37°C in 5% CO₂ for 15 minutes. This was repeated a minimum of three times to remove all bad and contracted fibers. Single fibers were then cultured in plating medium, PM (10% HS, 0.5% chick embryo extract [CEE; US Biological, Swampscott, MA]) in DMEM, for 1 day and then switched to proliferating medium (20%

Fetal Bovine Serum [FBS]; Mediatech, Herndon, VA), 10% HS, 2% CEE in DMEM)

Bulk prep for SCs isolation and primary culture

Hindlimb muscles were incubated in DMEM with 0.2% (w/v) collagenase II (Gibco BRL) for 90 minutes at 37°C. Digested muscle was then washed in rinsing buffer, RB (Ham's F-10 nutrient mixture with 10% HS) and dissociated into single myofibers by repeated triturating with a Pasteur pipette.

Myofiber fragments were centrifuged at 1500 rpm for 5 minutes, rinsed and incubated in RB, 0.2% collagenase II, 0.4% dispase at 37°C for 30 minutes. To release SCs from the fibers, samples were syringed four times, filtered through 40µm and 20µm filters and spinned at 1500 rpm for 5 minutes. Cell pellet was resuspended in Growth Medium (GM) (Ham's F-10 nutrient mixture with 20% FBS, 5 ng/ml basic fibroblast growth factor [R&D Systems, Minneapolis, MN], and 1% penicillin/streptomycin [Gibco BRL]) plated in 10 cm dishes coated with 1/1000 ECM and incubated at 37°C in 5% CO₂. SCs progenitors pure culture was enriched by pre-plating culture in order to avoid fibroblasts contamination. To generate "reserve cell" cultures [139], low passage primary myoblasts were maintained in GM and switched to differentiation media DM (3% HS in DMEM) for 3 days at high density (80-90% confluency). Cdk4/6 inhibitor IV (Calbiochem) was added to culture after adenovirus infection.

FLUORESCENT ACTIVATED CELL SORTING (FACS)

To obtain highly purified myogenic cells, mononucleated cells were isolated from uninjured and regenerating muscle as described [35, 140] with modifications. Bulk prepped SCs were incubated in biotinylated anti-vcam1 and anti mouse-integrin- α 7 for 45 minutes in sorting media (5% FBS, 10% Horse Serum in Hams F10), followed by a second incubation with CD31-PE, CD45-PE, Streptavidin Alexa647 and anti-mouse Alexa Pacific blue for 30 minutes. Cells were washed in sorting media and spun at 1500rpm for 5 minutes, resuspended in 500ul sorting media and filtered. Myogenic cells had the following profile: V-

CAM⁺, Integrin- α 7⁺, CD31⁻, CD45⁻, PI. Cells were sorted using FACS Aria (BD Biosciences). Sorted cells were collected for *in vitro* analysis or primary culture.

ACTIVATION OF Cre RECOMBINASE

Low passage myoblasts were infected with adenovirus Ad5CMVCre-eGFP or Ad5CMV-eGFP-control (Gene Transfer Vector Core, University of Iowa) diluted 1:1000 in GM from a stock titer of 1×10^{10} pfu/ml for 1.5 hr at 37°C. Cells were washed with PBS and incubated in fresh PM/GM for 18 hours or 24 hours and either fixed or replated in GM at equal density for 48 hours and switched to fusion media for 3 days. Mice aged 3-4 months were given intraperitoneal (i.p.) injection of tamoxifen (TM) (300 μ l, 10 mg/ml, diluted in corn oil [Sigma, St. Louis, MO] daily for 3 days).

HISTOLOGY AND IMMUNOFLUORESCENCE

Histology and immunofluorescence

TA muscles were dehydrated in 20% sucrose in PBS (Phosphate Buffered Saline) and placed in cryobox with O.C.T. for cryostat sectioning. Muscle section (10 μ m) were fixed in 4% PFA for 10 min at room temperature, permeabilized and incubated in blocking solution, BS (10% Goat Serum, PBS/ 0.2% TritonX-100 [PBST]) for 1 hour. Primary antibodies were incubated in BS overnight at 4°C. The day after muscle section were washed with PBST, incubated in BS for 30 minutes and in secondary antibodies for 1 hour at room temperature, in hydrated dark chamber. After several washes with PBST muscle sections were mounted and observed at fluorescence microscopy. Immunofluorescence was performed on fixed cells and fixed fibers (4% PFA, 10 minutes) after permeabilization (0.2% PBT; 10 min) and block (10% GS in PBT). Cells/fibers were incubated in primary antibodies overnight at 4°C. Cells/Fibers were washed and blocked in 10% GS/PBST then incubated in fluorophore-conjugated antibody and DAPI to visualize nuclei for 1 hour at room temperature.

REAL-TIME RT-PCR

Total RNA was extracted using TRIZOL® (Invitrogen) from FACS sorted cells and myoblasts collected respectively from either uninjured or regenerating muscle, or adenovirus infected myoblasts and prepared for qRT-PCR analysis. First-strand cDNA was directly synthesized from each cell lysate by the SuperScript® II Cells Direct cDNA Synthesis Kit (Invitrogen). Quantitative real-time PCR was performed with Platinum®SYBR®Green qPCR SuperMix-UDG with ROX (Invitrogen). Mouse Cell Cycle RT² Profiler™ PCR Array (Qiagen, SABiosciences) was performed on StepOne Plus Real Time System (Applied Biosystem) with RT² SYBR® green ROX™ qPCR Mastermix (Qiagen, SABioscience).

WESTERN BLOT

Primary myoblasts were harvested and lysed in RIPA extraction buffer (50mM Tris-HCl, pH 7.4. 1% NP-40, 0.5% sodium deoxycholate, 0.1% sodium dodecyl sulfate, 5mM EDTA, 150 mM NaCl and 50mM NaF) supplemented with protease and phosphatase inhibitors (complete; Roche). Western Blot were probed with antibodies listed in table...Secondary detection was performed with HRP-conjugated antibodies. Membrane-bound immune complexes were visualized by ECL kit (GE Healthcare, Amersham Biosciences).

SENESCENCE ASSAY

Cellular senescence assay was performed using Cellular Senescence Assay (Millipore) and following manufacturer's instruction.

STATISTICAL ANALYSIS

A minimum of 2 and up to 3 replicates was done for all experiments presented. Data are presented as means and standard errors of the mean. Comparisons between groups were done using a one way analysis of variance. Comparisons

within groups were done using a t-test with repeated measures. Differences were considered statistically significant at the $p < 0.05$ level.

ANTIBODIES

The source and concentration of antibodies: Rat anti-BrdU (1/500, Abcam), rabbit anti-ki67 (1/200, Abcam), mouse anti-Pax7 (1/100, DSHB), rabbit anti-MyoD (1/70 for immunohistochemistry, 1/200 for Western Blot, Santa Cruz), rabbit anti-Myogenin (1/200, Santa Cruz), mouse anti-BrdU (1/500), rabbit anti-Myf5 (1/200, Santa Cruz), chick anti-Laminin (1/5000, Abcam), chicken anti-GFP (1/500, Invitrogen), rabbit anti-P16 (1/200, Santa Cruz), rabbit anti-cyclin D1 (1/1000, Cell Signaling), rabbit anti-GAPDH (1:5000, Cell Signaling) mouse anti- α 7 integrin (1/200 for FACS, MBL), vcam biotin (1/200 for FACS, Novus Bio), CD31-PE and CD45-PE (1/200, BD). The corresponding species-specific Alexa-conjugated (488, 546, 647) secondary antibodies (Molecular Probes) were used at 1/2000 for immunohistochemistry or 1/200 for FACS, anti-mouse IgG, HRP-linked (1/2000, Cell Signaling), anti-rabbit IgG, HRP-linked (1/2000, Cell Signaling).

PRIMERS

P16 Fw gtgcgatatttgcttcc, Rev ctctgctcttgggattgg

P27 Fw aggcaaactctgaggaccggca, Rev tgctccacagtgccagcgttc

P57 Fw cgaggagcaggacgagaatc, Rev gaagaagtcgttcgcattggc

P21 Fw tggagtcaggcgcagatccac, Rev cgccatgagcgcacatcgcaatc

Cyclin D1 Fw gcgtaccctgacaccaatctctc Rev acctctcttcgcacttctgctcc

MyoD Fw cactacagtggcgactcagatgc Rev tgacacagccgcactcttc

Myogenin Fw ttgctcagctccctcaaccagg Rev tagggtcagccgcagcaaatg

Pax7 Fw gtggaatcagaacccgacctc Rev gtagtgggtcctctctcaaaggc

Myf5 Fw attacagcctgccgggacagag Rev gcaatccaagctggacacggag

GAPDH Fw agtgcggtgtgaacggattg, Rev tgtagaccatgtagttgaggtca

All reactions for Real time qPCR were performed using the following thermal cycler conditions: 50°C for 2 min, 95°C for 2 min followed by 40 cycles of a 3 step reaction; denaturation at 95°C for 15 sec, annealing at 60°C for 30 sec and extension and data collection at 72°C for 30 sec. All genes expression were normalized on GAPDH.

REFERENCES

1. Wigmore, P.M. and D.J. Evans, *Molecular and cellular mechanisms involved in the generation of fiber diversity during myogenesis*. *Int.Rev.Cytol.*, 2002. **216**: p. 175-232.
2. Tajbakhsh, S., *Skeletal muscle stem cells in developmental versus regenerative myogenesis*. *J Intern Med*, 2009. **266**(4): p. 372-89.
3. Bentzinger, C.F., J. von Maltzahn, and M.A. Rudnicki, *Extrinsic regulation of satellite cell specification*. *Stem Cell Res Ther*, 2010. **1**(3): p. 27.
4. Kwak, K.B., et al., *Increase in the level of m-calpain correlates with the elevated cleavage of filamin during myogenic differentiation of embryonic muscle cells*. *Biochim Biophys Acta*, 1993. **1175**(3): p. 243-9.
5. Coulton, G.R., et al., *The mdx mouse skeletal muscle myopathy: I. A histological, morphometric and biochemical investigation*. *Neuropathol Appl Neurobiol*, 1988. **14**(1): p. 53-70.
6. Konigsberg, I.R., *Clonal analysis of myogenesis*. *Science*, 1963. **140**: p. 1273-84.
7. Yaffe, D., *Cellular aspects of muscle differentiation in vitro*. *Curr Top Dev Biol*, 1969. **4**: p. 37-77.
8. Bischoff, R., *Regeneration of single skeletal muscle fibers in vitro*. *Anat.Rec.*, 1975. **182**(2): p. 215-235.
9. Collins, C.A., et al., *Stem cell function, self-renewal, and behavioral heterogeneity of cells from the adult muscle satellite cell niche*. *Cell*, 2005. **122**(2): p. 289-301.
10. Cerletti, M., et al., *Highly efficient, functional engraftment of skeletal muscle stem cells in dystrophic muscles*. *Cell*, 2008. **134**(1): p. 37-47.
11. Sacco, A., et al., *Self-renewal and expansion of single transplanted muscle stem cells*. *Nature*, 2008. **456**(7221): p. 502-506.
12. Whalen, R.G., et al., *Expression of myosin isoforms during notexin-induced regeneration of rat soleus muscles*. *Dev Biol*, 1990. **141**(1): p. 24-40.
13. Cerletti, M., et al., *Regulation and function of skeletal muscle stem cells*. *Cold Spring Harb Symp Quant Biol*, 2008. **73**: p. 317-22.
14. Charge, S.B. and M.A. Rudnicki, *Cellular and molecular regulation of muscle regeneration*. *Physiol Rev.*, 2004. **84**(1): p. 209-238.
15. Mauro, A., *Satellite cell of skeletal muscle fibers*. *J Biophys Biochem Cytol*, 1961. **9**: p. 493-5.
16. Buckingham, M., et al., *The formation of skeletal muscle: from somite to limb*. *J Anat*, 2003. **202**(1): p. 59-68.
17. Goulding, M., A. Lumsden, and A.J. Paquette, *Regulation of Pax-3 expression in the dermomyotome and its role in muscle development*. *Development*, 1994. **120**(4): p. 957-71.
18. Cossu, G., et al., *Activation of different myogenic pathways: myf-5 is induced by the neural tube and MyoD by the dorsal ectoderm in mouse paraxial mesoderm*. *Development*, 1996. **122**(2): p. 429-37.

19. Birchmeier, C. and H. Brohmann, *Genes that control the development of migrating muscle precursor cells*. *Curr Opin Cell Biol*, 2000. **12**(6): p. 725-30.
20. Relaix, F., et al., *A Pax3/Pax7-dependent population of skeletal muscle progenitor cells*. *Nature*, 2005. **435**(7044): p. 948-953.
21. Seale, P., et al., *Pax7 is required for the specification of myogenic satellite cells*. *Cell*, 2000. **102**(6): p. 777-786.
22. Relaix, F., et al., *Pax3 and Pax7 have distinct and overlapping functions in adult muscle progenitor cells*. *J.Cell Biol.*, 2006. **172**(1): p. 91-102.
23. Zammit, P.S., et al., *Pax7 and myogenic progression in skeletal muscle satellite cells*. *J.Cell Sci.*, 2006. **119**(Pt 9): p. 1824-1832.
24. Olguin, H.C., et al., *Reciprocal inhibition between Pax7 and muscle regulatory factors modulates myogenic cell fate determination*. *J.Cell Biol.*, 2007. **177**(5): p. 769-779.
25. Seale, P., et al., *Muscle satellite cell-specific genes identified by genetic profiling of MyoD-deficient myogenic cell*. *Dev.Biol.*, 2004. **275**(2): p. 287-300.
26. Lepper, C., S.J. Conway, and C.M. Fan, *Adult satellite cells and embryonic muscle progenitors have distinct genetic requirements 2*. *Nature*, 2009. **460**(7255): p. 627-631.
27. Schienda, J., et al., *Somitic origin of limb muscle satellite and side population cells*. *Proc.Natl.Acad.Sci.U.S.A*, 2006. **103**(4): p. 945-950.
28. Kanisicak, O., et al., *Progenitors of skeletal muscle satellite cells express the muscle determination gene, MyoD*. *Dev.Biol.*, 2009.
29. Brack, A., *Adult muscle stem cells avoid death and Paxes*. *Cell Stem Cell*, 2009. **5**(2): p. 132-134.
30. Bischoff, R. and C. Heintz, *Enhancement of skeletal muscle regeneration*. *Dev.Dyn.*, 1994. **201**(1): p. 41-54.
31. Schultz, E., M.C. Gibson, and T. Champion, *Satellite cells are mitotically quiescent in mature mouse muscle: an EM and radioautographic study*. *J.Exp.Zool.*, 1978. **206**(3): p. 451-456.
32. Rudnicki, M.A., et al., *The molecular regulation of muscle stem cell function*. *Cold Spring Harb.Symp.Quant.Biol.*, 2008. **73**: p. 323-331.
33. Kuang, S., et al., *Asymmetric self-renewal and commitment of satellite stem cells in muscle*. *Cell*, 2007. **129**(5): p. 999-1010.
34. Tanaka, K.K., et al., *Syndecan-4-expressing muscle progenitor cells in the SP engraft as satellite cells during muscle regeneration*. *Cell Stem Cell*, 2009. **4**(3): p. 217-225.
35. Shea, K.L., et al., *Sprouty1 regulates reversible quiescence of a self-renewing adult muscle stem cell pool during regeneration*. *Cell Stem Cell*. **6**(2): p. 117-129.
36. Ferrari, G., et al., *Muscle regeneration by bone marrow-derived myogenic progenitors*. *Science*, 1998. **279**(5356): p. 1528-30.
37. Gussoni, E., et al., *Dystrophin expression in the mdx mouse restored by stem cell transplantation*. *Nature*, 1999. **401**(6751): p. 390-4.
38. Sampaolesi, M., et al., *Cell therapy of alpha-sarcoglycan null dystrophic mice through intra-arterial delivery of mesoangioblasts*. *Science*, 2003. **301**(5632): p. 487-92.
39. Dellavalle, A., et al., *Pericytes of human skeletal muscle are myogenic precursors distinct from satellite cells*. *Nat Cell Biol*, 2007. **9**(3): p. 255-67.
40. Dellavalle, A., et al., *Pericytes resident in postnatal skeletal muscle differentiate into muscle fibres and generate satellite cells*. *Nat Commun*, 2011. **2**: p. 499.

41. Torrente, Y., et al., *Human circulating AC133(+) stem cells restore dystrophin expression and ameliorate function in dystrophic skeletal muscle*. J.Clin.Invest, 2004. **114**(2): p. 182-195.
42. Mitchell, K.J., et al., *Identification and characterization of a non-satellite cell muscle resident progenitor during postnatal development*. Nat Cell Biol, 2010. **12**(3): p. 257-66.
43. Joe, A.W., et al., *Muscle injury activates resident fibro/adipogenic progenitors that facilitate myogenesis*. Nat Cell Biol, 2010. **12**(2): p. 153-63.
44. Sambasivan, R., et al., *Pax7-expressing satellite cells are indispensable for adult skeletal muscle regeneration*. Development, 2011. **138**(17): p. 3647-56.
45. Lepper, C., T.A. Partridge, and C.M. Fan, *An absolute requirement for Pax7-positive satellite cells in acute injury-induced skeletal muscle regeneration*. Development, 2011. **138**(17): p. 3639-46.
46. Murphy, M.M., et al., *Satellite cells, connective tissue fibroblasts and their interactions are crucial for muscle regeneration*. Development, 2011. **138**(17): p. 3625-37.
47. Rudnicki, M.A. and R. Jaenisch, *The MyoD family of transcription factors and skeletal myogenesis*. Bioessays, 1995. **17**(3): p. 203-9.
48. Olguin, H.C. and B.B. Olwin, *Pax-7 up-regulation inhibits myogenesis and cell cycle progression in satellite cells: a potential mechanism for self-renewal*. Dev.Biol., 2004. **275**(2): p. 375-388.
49. Halevy, O., et al., *Pattern of Pax7 expression during myogenesis in the posthatch chicken establishes a model for satellite cell differentiation and renewal*. Dev.Dyn., 2004. **231**(3): p. 489-502.
50. Yamada, M., et al., *High concentrations of HGF inhibit skeletal muscle satellite cell proliferation in vitro by inducing expression of myostatin: a possible mechanism for reestablishing satellite cell quiescence in vivo*. Am.J.Physiol Cell Physiol. **298**(3): p. C465-C476.
51. Abou-Khalil, R., et al., *Autocrine and paracrine angiopoietin 1/Tie-2 signaling promotes muscle satellite cell self-renewal*. Cell Stem Cell, 2009. **5**(3): p. 298-309.
52. Conboy, I.M. and T.A. Rando, *The regulation of Notch signaling controls satellite cell activation and cell fate determination in postnatal myogenesis*. Dev.Cell, 2002. **3**(3): p. 397-409.
53. Fukada, S., et al., *Molecular signature of quiescent satellite cells in adult skeletal muscle*. Stem Cells, 2007. **25**(10): p. 2448-2459.
54. Brack, A.S., et al., *A temporal switch from notch to Wnt signaling in muscle stem cells is necessary for normal adult myogenesis*. Cell Stem Cell, 2008. **2**(1): p. 50-59.
55. Hawke, T.J. and D.J. Garry, *Myogenic satellite cells: physiology to molecular biology*. J.Appl.Physiol, 2001. **91**(2): p. 534-551.
56. Abou-Khalil, R. and A.S. Brack, *Muscle stem cells and reversible quiescence: the role of sprouty*. Cell Cycle, 2010. **9**(13): p. 2575-80.
57. Jang, Y.C., et al., *Skeletal Muscle Stem Cells: Effects of Aging and Metabolism on Muscle Regenerative Function*. Cold Spring Harb Symp Quant Biol, 2011.
58. Brack, A.S., H. Bildsoe, and S.M. Hughes, *Evidence that satellite cell decrement contributes to preferential decline in nuclear number from large fibres during murine age-related muscle atrophy*. J.Cell Sci., 2005. **118**(Pt 20): p. 4813-4821.
59. Conboy, I.M., et al., *Notch-mediated restoration of regenerative potential to aged muscle*. Science, 2003. **302**(5650): p. 1575-1577.

60. Sharpless, N.E. and R.A. DePinho, *Telomeres, stem cells, senescence, and cancer*. J Clin Invest, 2004. **113**(2): p. 160-8.
61. Pasinelli, P. and R.H. Brown, *Molecular biology of amyotrophic lateral sclerosis: insights from genetics*. Nat Rev Neurosci, 2006. **7**(9): p. 710-23.
62. Boillee, S., C. Vande Velde, and D.W. Cleveland, *ALS: a disease of motor neurons and their nonneuronal neighbors*. Neuron, 2006. **52**(1): p. 39-59.
63. Boillee, S., et al., *Onset and progression in inherited ALS determined by motor neurons and microglia*. Science, 2006. **312**(5778): p. 1389-92.
64. Gonzalez de Aguilar, J.L., et al., *Amyotrophic lateral sclerosis: all roads lead to Rome*. J Neurochem, 2007. **101**(5): p. 1153-60.
65. Rosen, D.R., *Mutations in Cu/Zn superoxide dismutase gene are associated with familial amyotrophic lateral sclerosis*. Nature, 1993. **364**(6435): p. 362.
66. Cleveland, D.W. and J.D. Rothstein, *From Charcot to Lou Gehrig: deciphering selective motor neuron death in ALS*. Nat Rev Neurosci, 2001. **2**(11): p. 806-19.
67. Clement, A.M., et al., *Wild-type nonneuronal cells extend survival of SOD1 mutant motor neurons in ALS mice*. Science, 2003. **302**(5642): p. 113-7.
68. Dobrowolny, G., et al., *Skeletal muscle is a primary target of SOD1G93A-mediated toxicity*. Cell Metab, 2008. **8**(5): p. 425-36.
69. Dupuis, L. and J.P. Loeffler, *Neuromuscular junction destruction during amyotrophic lateral sclerosis: insights from transgenic models*. Curr Opin Pharmacol, 2009. **9**(3): p. 341-6.
70. Lino, M.M., C. Schneider, and P. Caroni, *Accumulation of SOD1 mutants in postnatal motoneurons does not cause motoneuron pathology or motoneuron disease*. J Neurosci, 2002. **22**(12): p. 4825-32.
71. Pramatarova, A., et al., *Neuron-specific expression of mutant superoxide dismutase 1 in transgenic mice does not lead to motor impairment*. J Neurosci, 2001. **21**(10): p. 3369-74.
72. Jaarsma, D., et al., *Neuron-specific expression of mutant superoxide dismutase is sufficient to induce amyotrophic lateral sclerosis in transgenic mice*. J Neurosci, 2008. **28**(9): p. 2075-88.
73. Bouteloup, C., et al., *Hypermetabolism in ALS patients: an early and persistent phenomenon*. J Neurol, 2009. **256**(8): p. 1236-42.
74. Dupuis, L., et al., *Evidence for defective energy homeostasis in amyotrophic lateral sclerosis: benefit of a high-energy diet in a transgenic mouse model*. Proc Natl Acad Sci U S A, 2004. **101**(30): p. 11159-64.
75. Dupuis, L., et al., *Nogo provides a molecular marker for diagnosis of amyotrophic lateral sclerosis*. Neurobiol Dis, 2002. **10**(3): p. 358-65.
76. Wong, M. and L.J. Martin, *Skeletal muscle-restricted expression of human SOD1 causes motor neuron degeneration in transgenic mice*. Hum Mol Genet, 2010. **19**(11): p. 2284-302.
77. Williams, A.H., et al., *MicroRNA-206 delays ALS progression and promotes regeneration of neuromuscular synapses in mice*. Science, 2009. **326**(5959): p. 1549-54.
78. Funakoshi, H., et al., *Muscle-derived neurotrophin-4 as an activity-dependent trophic signal for adult motor neurons*. Science, 1995. **268**(5216): p. 1495-9.
79. Kablar, B. and M.A. Rudnicki, *Development in the absence of skeletal muscle results in the sequential ablation of motor neurons from the spinal cord to the brain*. Dev Biol, 1999. **208**(1): p. 93-109.
80. Jirmanova, I. and S. Thesleff, *Ultrastructural study of experimental muscle degeneration and regeneration in the adult rat*. Z Zellforsch Mikrosk Anat, 1972. **131**(1): p. 77-97.

81. Grubb, B.D., J.B. Harris, and I.S. Schofield, *Neuromuscular transmission at newly formed neuromuscular junctions in the regenerating soleus muscle of the rat*. J Physiol, 1991. **441**: p. 405-21.
82. Pradat, P.F., et al., *Abnormalities of satellite cells function in amyotrophic lateral sclerosis*. Amyotroph Lateral Scler, 2011. **12**(4): p. 264-71.
83. Kitzmann, M. and A. Fernandez, *Crosstalk between cell cycle regulators and the myogenic factor MyoD in skeletal myoblasts*. Cell Mol.Life Sci., 2001. **58**(4): p. 571-579.
84. Blomen, V.A. and J. Boonstra, *Cell fate determination during G1 phase progression*. Cell Mol.Life Sci., 2007. **64**(23): p. 3084-3104.
85. Dehay, C. and H. Kennedy, *Cell-cycle control and cortical development*. Nat Rev Neurosci, 2007. **8**(6): p. 438-50.
86. Wei, Q. and B.M. Paterson, *Regulation of MyoD function in the dividing myoblast*. FEBS Lett, 2001. **490**(3): p. 171-8.
87. Kim, W.Y. and N.E. Sharpless, *The regulation of INK4/ARF in cancer and aging*. Cell, 2006. **127**(2): p. 265-275.
88. Sharpless, N.E., *INK4a/ARF: a multifunctional tumor suppressor locus*. Mutat Res, 2005. **576**(1-2): p. 22-38.
89. Huh, M.S., et al., *Rb is required for progression through myogenic differentiation but not maintenance of terminal differentiation*. J Cell Biol, 2004. **166**(6): p. 865-76.
90. Hosoyama, T., et al., *Rb1 gene inactivation expands satellite cell and postnatal myoblast pools*. J Biol Chem, 2011. **286**(22): p. 19556-64.
91. Campisi, J., et al., *Cellular senescence: A link between cancer and age-related degenerative disease?* Semin Cancer Biol, 2011. **21**(6): p. 354-9.
92. Sharpless, N.E. and R.A. DePinho, *How stem cells age and why this makes us grow old*. Nat Rev Mol Cell Biol, 2007. **8**(9): p. 703-13.
93. Baker, D.J., et al., *Clearance of p16Ink4a-positive senescent cells delays ageing-associated disorders*. Nature, 2011. **479**(7372): p. 232-6.
94. Janzen, V., et al., *Stem-cell ageing modified by the cyclin-dependent kinase inhibitor p16INK4a*. Nature, 2006. **443**(7110): p. 421-426.
95. Krishnamurthy, J., et al., *p16INK4a induces an age-dependent decline in islet regenerative potential*. Nature, 2006. **443**(7110): p. 453-7.
96. Chen, H., et al., *Polycomb protein Ezh2 regulates pancreatic beta-cell Ink4a/Arf expression and regeneration in diabetes mellitus*. Genes Dev, 2009. **23**(8): p. 975-85.
97. Molofsky, A.V., et al., *Increasing p16INK4a expression decreases forebrain progenitors and neurogenesis during ageing*. Nature, 2006. **443**(7110): p. 448-452.
98. Krishnamurthy, J., et al., *p16INK4a induces an age-dependent decline in islet regenerative potential*. Nature, 2006. **443**(7110): p. 453-457.
99. Baker, D.J., et al., *Opposing roles for p16Ink4a and p19Arf in senescence and ageing caused by BubR1 insufficiency*. Nat Cell Biol, 2008. **10**(7): p. 825-36.
100. Lal, A., et al., *p16(INK4a) translation suppressed by miR-24*. PLoS One, 2008. **3**(3): p. e1864.
101. Caretti, G., et al., *The Polycomb Ezh2 methyltransferase regulates muscle gene expression and skeletal muscle differentiation*. Genes Dev, 2004. **18**(21): p. 2627-38.
102. Juan, A.H., et al., *Polycomb EZH2 controls self-renewal and safeguards the transcriptional identity of skeletal muscle stem cells*. Genes Dev, 2011. **25**(8): p. 789-94.

103. Park, I.K., et al., *Bmi-1 is required for maintenance of adult self-renewing haematopoietic stem cells*. Nature, 2003. **423**(6937): p. 302-5.
104. Molofsky, A.V., et al., *Bmi-1 dependence distinguishes neural stem cell self-renewal from progenitor proliferation*. Nature, 2003. **425**(6961): p. 962-7.
105. Sauvageau, M. and G. Sauvageau, *Polycomb group proteins: multi-faceted regulators of somatic stem cells and cancer*. Cell Stem Cell, 2010. **7**(3): p. 299-313.
106. Akasaka, T., et al., *Mice doubly deficient for the Polycomb Group genes *Mel18* and *Bmi1* reveal synergy and requirement for maintenance but not initiation of *Hox* gene expression*. Development, 2001. **128**(9): p. 1587-97.
107. Robson, L.G., et al., *Bmi1 is expressed in postnatal myogenic satellite cells, controls their maintenance and plays an essential role in repeated muscle regeneration*. PLoS One, 2011. **6**(11): p. e27116.
108. Liu, Y. and N.E. Sharpless, *Tumor suppressor mechanisms in immune aging*. Curr Opin Immunol, 2009. **21**(4): p. 431-9.
109. Campisi, J., *Cellular senescence: putting the paradoxes in perspective*. Curr Opin Genet Dev, 2011. **21**(1): p. 107-12.
110. Corbu, A., et al., *Satellite cell characterization from aging human muscle*. Neurol Res, 2010. **32**(1): p. 63-72.
111. Viguie, C.A., et al., *Quantitative study of the effects of long-term denervation on the extensor digitorum longus muscle of the rat*. Anat Rec, 1997. **248**(3): p. 346-54.
112. Dedkov, E.I., et al., *Reparative myogenesis in long-term denervated skeletal muscles of adult rats results in a reduction of the satellite cell population*. Anat Rec, 2001. **263**(2): p. 139-54.
113. Deato, M.D., et al., *MyoD targets TAF3/TRF3 to activate myogenin transcription*. Mol Cell, 2008. **32**(1): p. 96-105.
114. Brack, A.S. and T.A. Rando, *Intrinsic changes and extrinsic influences of myogenic stem cell function during aging*. Stem Cell Rev., 2007. **3**(3): p. 226-237.
115. Monahan, K.B., et al., *Somatic p16(*INK4a*) loss accelerates melanomagenesis*. Oncogene, 2010. **29**(43): p. 5809-17.
116. Sherr, C.J. and J.M. Roberts, *CDK inhibitors: positive and negative regulators of G1-phase progression*. Genes Dev, 1999. **13**(12): p. 1501-12.
117. Nishijo, K., et al., *Biomarker system for studying muscle, stem cells, and cancer in vivo*. FASEB J., 2009.
118. Valk-Lingbeek, M.E., S.W. Bruggeman, and M. van Lohuizen, *Stem cells and cancer; the polycomb connection*. Cell, 2004. **118**(4): p. 409-18.
119. Gil, J., D. Bernard, and G. Peters, *Role of polycomb group proteins in stem cell self-renewal and cancer*. DNA Cell Biol, 2005. **24**(2): p. 117-25.
120. Jacobs, J.J., et al., *The oncogene and Polycomb-group gene *bmi-1* regulates cell proliferation and senescence through the *ink4a* locus*. Nature, 1999. **397**(6715): p. 164-168.
121. Lessard, J. and G. Sauvageau, *Bmi-1 determines the proliferative capacity of normal and leukaemic stem cells*. Nature, 2003. **423**(6937): p. 255-60.
122. Hosen, N., et al., *Bmi-1-green fluorescent protein-knock-in mice reveal the dynamic regulation of *bmi-1* expression in normal and leukemic hematopoietic cells*. Stem Cells, 2007. **25**(7): p. 1635-44.
123. Collins, C.J. and J.M. Sedivy, *Involvement of the *INK4a/Arf* gene locus in senescence*. Aging Cell, 2003. **2**(3): p. 145-50.
124. Campisi, J., *Suppressing cancer: the importance of being senescent*. Science, 2005. **309**(5736): p. 886-7.

125. Krishnamurthy, J., et al., *Ink4a/Arf expression is a biomarker of aging*. J.Clin.Invest, 2004. **114**(9): p. 1299-1307.
126. Bulavin, D.V. and A.J. Fornace, Jr., *p38 MAP kinase's emerging role as a tumor suppressor*. Adv Cancer Res, 2004. **92**: p. 95-118.
127. Zhang, P., et al., *p21(CIP1) and p57(KIP2) control muscle differentiation at the myogenin step*. Genes Dev, 1999. **13**(2): p. 213-24.
128. Reynaud, E.G., et al., *p57(Kip2) stabilizes the MyoD protein by inhibiting cyclin E-Cdk2 kinase activity in growing myoblasts*. Mol Cell Biol, 1999. **19**(11): p. 7621-9.
129. Vaccarello, G., et al., *p57Kip2 is induced by MyoD through a p73-dependent pathway*. J Mol Biol, 2006. **356**(3): p. 578-88.
130. Conboy, M.J., A.O. Karasov, and T.A. Rando, *High incidence of non-random template strand segregation and asymmetric fate determination in dividing stem cells and their progeny*. PLoS.Biol., 2007. **5**(5): p. e102.
131. Shinin, V., B. Gayraud-Morel, and S. Tajbakhsh, *Template DNA-strand cosegregation and asymmetric cell division in skeletal muscle stem cells*. Methods Mol.Biol., 2009. **482**: p. 295-317.
132. Conboy, I.M., et al., *Rejuvenation of aged progenitor cells by exposure to a young systemic environment*. Nature, 2005. **433**(7027): p. 760-764.
133. Carlson, M.E., M. Hsu, and I.M. Conboy, *Imbalance between pSmad3 and Notch induces CDK inhibitors in old muscle stem cells*. Nature, 2008. **454**(7203): p. 528-532.
134. Palacios, D., et al., *TNF/p38alpha/polycomb signaling to Pax7 locus in satellite cells links inflammation to the epigenetic control of muscle regeneration*. Cell Stem Cell, 2010. **7**(4): p. 455-69.
135. Chen, J.F., et al., *microRNA-1 and microRNA-206 regulate skeletal muscle satellite cell proliferation and differentiation by repressing Pax7*. J Cell Biol, 2010. **190**(5): p. 867-79.
136. Perry, R.L. and M.A. Rudnick, *Molecular mechanisms regulating myogenic determination and differentiation*. Front Biosci, 2000. **5**: p. D750-67.
137. Hawke, T.J., et al., *p21 is essential for normal myogenic progenitor cell function in regenerating skeletal muscle*. Am J Physiol Cell Physiol, 2003. **285**(5): p. C1019-27.
138. Kotake, Y., et al., *pRB family proteins are required for H3K27 trimethylation and Polycomb repression complexes binding to and silencing p16INK4alpha tumor suppressor gene*. Genes Dev, 2007. **21**(1): p. 49-54.
139. Yoshida, N., et al., *Cell heterogeneity upon myogenic differentiation: down-regulation of MyoD and Myf-5 generates 'reserve cells'*. J.Cell Sci., 1998. **111** (Pt 6): p. 769-779.
140. Brack, A.S., et al., *BCL9 is an essential component of canonical Wnt signaling that mediates the differentiation of myogenic progenitors during muscle regeneration*. Dev.Biol., 2009.

ACKNOWLEDGEMENTS

Three long years of PhD... moments of failures compensated by great successes, long experiments, infinite days spent at the bench or reading papers, preparing journal clubs and presentations...

Now, at the end of this chapter of my life, I believe that all these bad and good things made me strong and determined enough to keep going on this difficult, but so fascinating long way of science...Therefore, a first special thanks is to myself!!!

Along this way, I met a lot of people, that contribute to make this PhD special and very important for my scientific carrier and for my life.

Therefore, I would like to thank first of all Professor Lucio Cocco, coordinator of my PhD, for giving me the opportunity to participate in this PhD program, Professor Giovanna Cenacchi for always helping and supporting me during these long years and Dr Pasquale Chieco, director of CRBA, for trusting in my capacities. Moreover, I want to thank all of them for letting me do this important scientific experience in the USA.

When I started my PhD, I never expected to end it here in Boston, in such a great scientific environment. However, this became real thanks to my boss Dr Andrew Brack. I would like to express my sincere gratitude to him for giving me the opportunity to join his great lab and for teaching me all the secrets about science and the world of satellite cells. His guidance helped me during the time of research here at the Center for Regenerative Medicine and during the writing of this thesis. Moreover, he gave me continuous support for my PhD study and research, with patience, motivation, enthusiasm, and immense knowledge.

Then, I would like to thank the whole Andrew Brack's Lab, or it is better to say BARCLUB!! Thank you to all my crazy lab mates, in particular...Gstick to keeping organized our barclub with the "too bee doo list" and the "weekly motivational board", and to be always so helpful...GRAZIE per tutto quello che hai fatto per me dal primo giorno che sono arrivata, love you!!! Thanks to Kierandubidu....WHO IS?? My English teacher from London...Kieran thanks for "anything", you are marvelous and I wish you all the best in London..."Go Big or Go Home" that's what he said!!! I will miss our disco club in the scope room!!! Then, Swapniduuuu...thanks for helping me with your "steady and slow" philosophy...Thanks to Juisy, for the Danish Efficiency and a particular thanks is for Joe, or chakkaboom!! Joe, you are a great PostDoc and great person, I really learnt a lot from you...Thanks for your important scientific suggestion and discussion! I would also thank Rana Abou-Khalil and Eri Taniguchi, ex Post Doc in the lab, for contributing to some important data of my project. Thanks all of you guys, you are great scientist and it is a pleasure to work and collaborate with you!

A very special thanks, the most important, goes to my family...Even if far away you are always here, supporting me...I miss you a lot!! Grazie Mamma, Papà e la mia Ciccina per tutto quello che avete fatto e continuate sempre a fare per me... siete la mia vita...vi voglio bene!!

During this experience here in Boston, I met a lot of people and I would like to thanks everyone! But some of them contributed significantly to the realization of this chapter of my life!! A super special thanks is for my Sfrizzy...since we met in front of the Penthouse that night, we were always together sharing the bad and the good moment of this city, where pieces are missing, where rules can be reverted and invented, where nothing is predictable...I was very lucky to meet you in this great experience...we did a lot together and more we will do in the future...Ti voglio bene!!

Then, a Respectful thanks is for "THE Family"...La Famiggggggla... THANKS and RESPECT to Giacomo, Pietro, Nanni and il Sardo (per gli stupendi

rituali...daje!!!), Serena, Karin, Nada, I Pelati (Andrea e Gianluca), Serafino and his ants, Loredana (for more than just a WB support!!!) and Giuliano, Chiara and Ryan thanks all of you for the great moment in the House of Freedom and Thanks to everybody in the “Italian Community” here in Boston!

Thanks Laura for supporting me before and now that you are here, I still can't believe it...thanks for everything Ti voglio bene!

Thank you Rimba...even if just arrived two months are enough to appreciate you and your pearls of wisdom!!

Another special thanks is also for Pax...you trusted and supported me!!!

Thanks for my roommates Diana and Youmna, to be nice and very patient during these last months!

Even if now I am here, my heart is still in Italy with my friends...Ale, Assu, Sara, Eli thank you for the long-distance support and to be always present in my life...Nothing has changed, it is just a matter of distance...Right!?!

Sere, my dear Chemiche, thank you for trying every Sunday to make a Skype call, with your bad camera and internet connection....I love you and thanks to be always, always with me, you are very special and one day we will back to dance together!!!

Thanks also to my old lab mates and their special contribution to my scientific and life experience! Tony, Mauri, Cessa, Daniela, Valeria, Giulia, Marianna, Milena, Agent Pope... thank you all for being always good colleagues and friends!

Thank you everyone for making all these three years so special and important and let this dream become true... I will never forget!